

Università di Pisa  
LM Materials and Nanotechnology - a.a. 2016/17

## Spectroscopy of Nanomaterials II sem – part 9

Version 0, May 2017  
Francesco Fuso, francesco.fuso@unipi.it  
<http://www.df.unipi.it/~fuso/dida>

# Scanning Probe Microscopy: general concepts, STM, AFM

# OUTLOOK

In the provision to analyze an optical spectroscopy method based on a (specific) scanning probe, we move now towards a short and concise description of a couple of famous scanning probe microscopy techniques (and a few variants)

For the moment, we thus leave optics and related issues, and we concentrate on the microscopy (or nanoscopy) enabled by such techniques

Not to say, we will gain an insight into very well known and diffused (AFM, at least) methods which, since their introduction, have revolutionized microscopy

Today's menu:

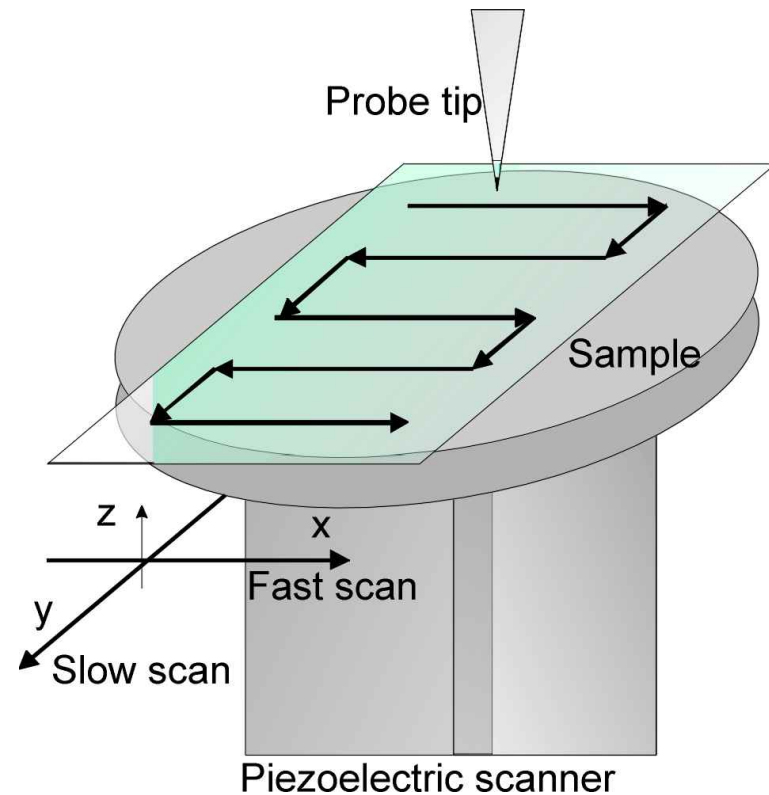
- General concepts of SPM, as starter
- First course of tunneling and STM, flavored with some examples
- Main course of atomic force and AFM, garnished with some fresh variant
- No dessert included

# SCANNING PROBE MICROSCOPY

**Scanning:** piezoelectric translator  
**Probe:** tip probing local properties  
**Microscopy:** sub-micrometer resolution  
(+ system to control tip/sample distance  
+ electronics for instrument operation)

Developed starting since '80s thanks to technical advancements leading to:

- ✓ Piezo translators with sub-nm resolution
- ✓ sub-nm probes

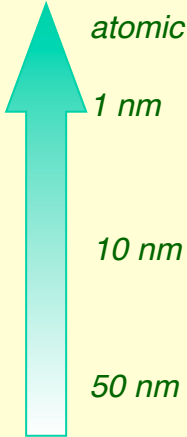


**Various physical quantities can be measured point-by-point during the scan and an image (i.e., a map of the quantity) can be built up**

***A topography map is almost always built during the scan***

# A HUGE VARIETY

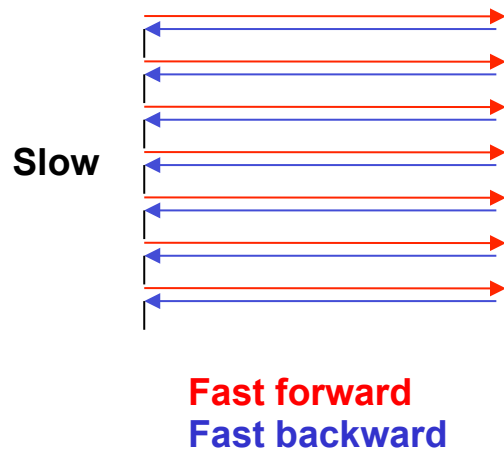
Technique	Probed quantity	Resolution
SFM	STM	Electron tunneling
	AFM	Mechanical force
	SFFM	Friction force
	MFM	Local magnetization
	EFM	Local polarization
	SNOM	Optical properties
...	...	...



Depending on the probe and on its interaction with the surface, a variety of physical effects can be investigated

*Typically, quantitative maps are obtained*

# RASTER SCAN



Normally, a  **raster scan** is applied:

- Scan addresses an array of discrete, equispaced “pixels” (e.g., 128x128, 256x256,...);
- Scan speed is different for one and the other directions (**fast and slow** scans, respectively);
- **Forward** (trace) and **backward** (retrace) scans along the “fast axis” are typically acquired;
- Forward/backward **comparison** is routinely used to assess the scan quality (unless it is used to derive some physical quantity, as in LFM)

The acquisition speeds is typically small, depending on:

- Time response of the scanner (typically a few ms for nm-sized displacements);
- The signal-to-noise of the quantity to be probed and acquired (through ms to s depending on the nature of the measurement and the related need to improve signal-to-noise)

Rule of thumb: scans are slow, because of the translator inertia and, mostly, of the weak signals to be acquired, requiring long integration times

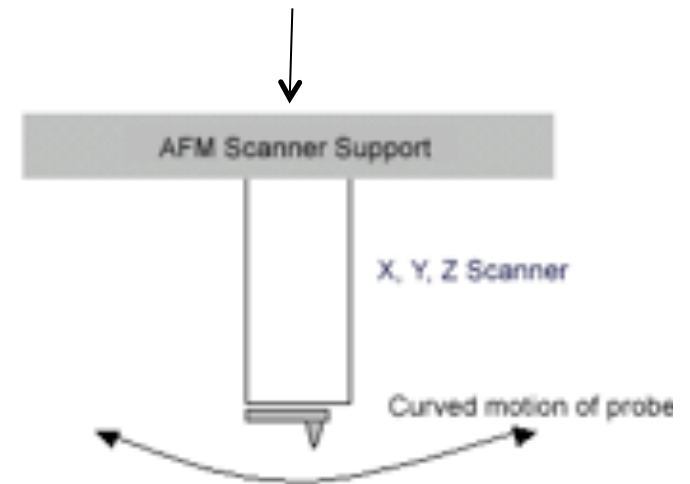
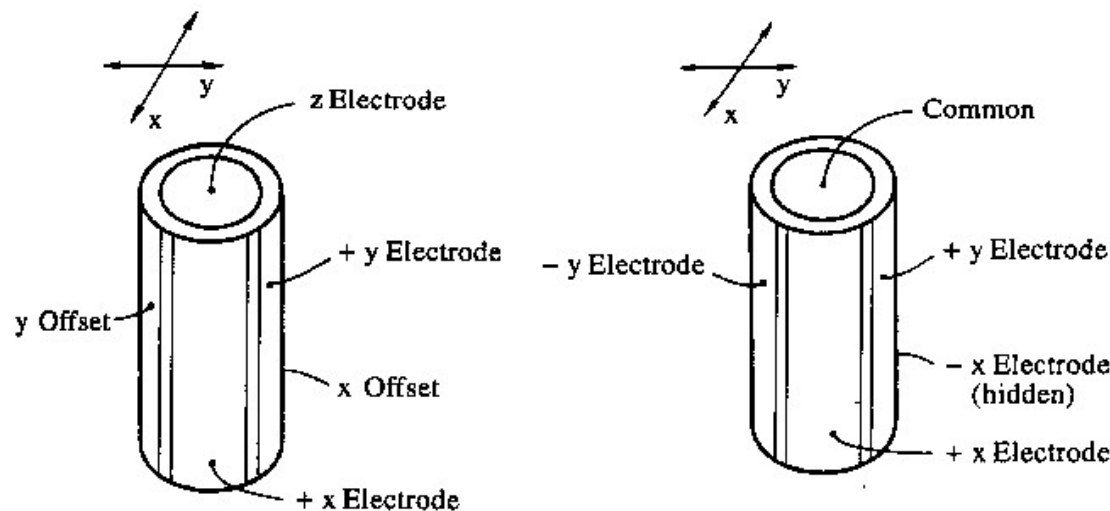
Exceptions: when atomic resolution is required (when enabled by the technique!), fast scans are used to prevent thermal drifts

# PIEZOELECTRIC TRANSLATORS I

The development of piezoelectric translator able to drive the position of the sample relative to the tip in all 3 directions has been a key point in the diffusion of SPMs

The simplest translator consists of an hollow piezoelectric cylinder:

- Suitably shaped electrodes enable application of electric fields in different sectors of the cylinder thickness
- A single hollow cylinder permits displacements along the three directions through deformation of the cylindrical shape
- ***There is some crosstalk between different directions, yet, as well as distortions***

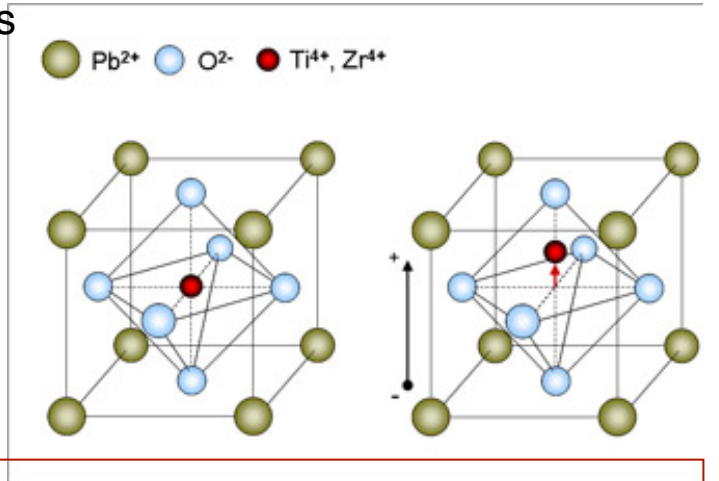


# PIEZOELECTRIC TRANSLATORS II

Typically, the piezoelectric material is PZT (lead zirconate titanate) ceramics

Main issues:

- Linearity (possibly closed loop)
- Hysteresis



Displacement along one direction:

$$\Delta t = d_{33} V .$$

$$d_{33} = 250 \cdot 10^{-12} \text{ m/V} , \quad d_{31} = -110 \cdot 10^{-12} \text{ m/V} ;$$

Nowadays: much more evolved piezoscanner with closed-loop operation (linear, self-calibrated displacements with pm accuracy!)

Displacement as small as  $\sim 0.1\text{-}0.5 \text{ nm/V}$  (along Z) are possible

Typical “scanner sensitivity”:

$\sim 1\text{-}10 \text{ nm/V}$  (along Z)

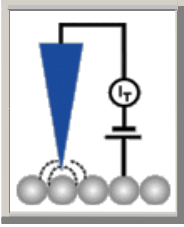
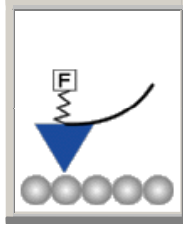
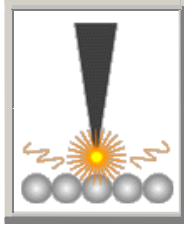
$\sim 1\text{-}100 \text{ nm/V}$  (along XY)

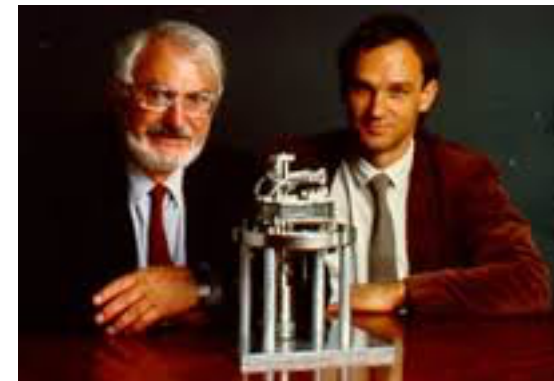
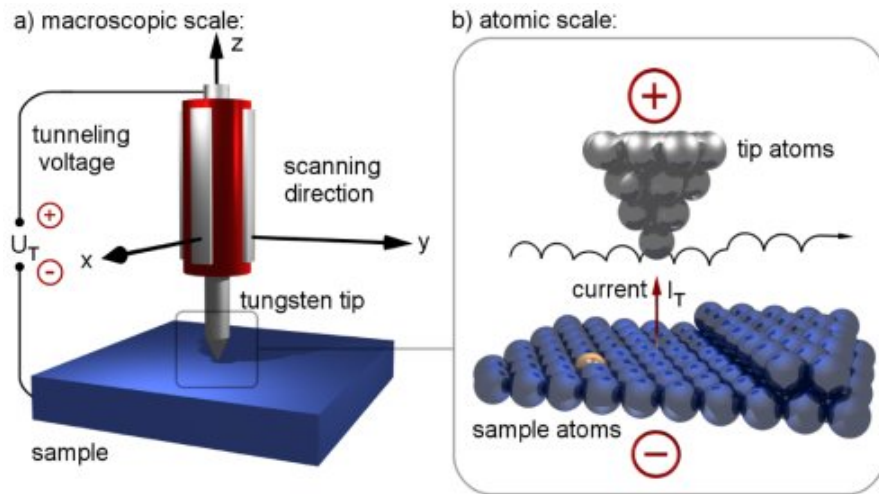
Typical driving voltages up to  $\pm 250 \text{ V}$

Typical min driving step size (16 bit)  $\sim 10 \text{ mV}$



# TUNNELING MICROSCOPY

		
<b>STM</b>	<b>AFM</b>	<b>SNOM</b>
<b>Electron tunneling</b>	<b>Force microscopy</b>	<b>Optical near-field</b>
<b>Locally probed quantity</b>		



G. Binnig, H. Rohrer, Nobel Prize in Physics 1986 for the Scanning Tunneling Microscope (STM)

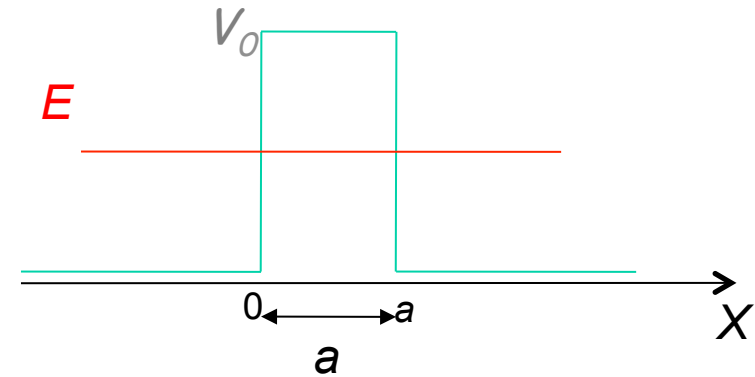


## REMINDERS ON THE TUNNEL EFFECT

A particle with (kinetic) energy  $E$  impinges onto a potential barrier with  $V_0 > E$

Classically, the particle is reflected back

**According to QM. particle can penetrate into the barrier and be transmitted across**



**Tunneling** occurs if  $a < \lambda_{dB} = k/2\pi = p/h = \sqrt{2mE}$

We search for an eigenfunction  $\psi(x)$  solution of the Schroedinger steady state equation

$$\text{for } x < 0: \quad \psi(x) = Ae^{ik_1x} + Be^{-ik_1x}$$

$$\text{for } x > a: \quad \psi(x) = Ce^{ik_1x} + De^{-ik_1x}$$

$$\text{with } k_1 = \frac{\sqrt{2mE}}{\hbar} \quad (\text{free particle})$$

$$\text{for } 0 < x < a: \quad \psi(x) = Fe^{ik_2x} + Ge^{-ik_2x}$$

$$\text{with } k_2 = \frac{\sqrt{2m(E - V_0)}}{\hbar} \quad \text{imaginary}$$



$$\text{for } 0 < x < a: \quad \psi(x) = Fe^{-k_3x} + Ge^{k_3x}$$

$$\text{with } k_3 = \frac{\sqrt{2m(V_0 - E)}}{\hbar} = \frac{k_2}{i} \quad \text{real}$$

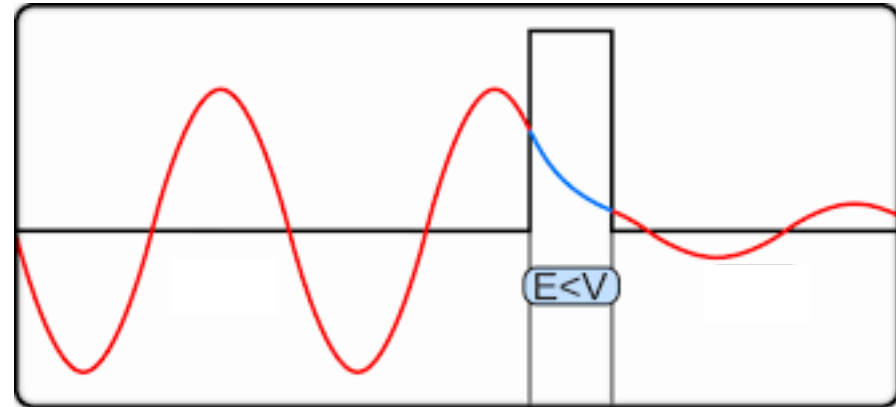
# EXPONENTIAL DECAY

Would lead to an exponential increase, not compatible with "energy conservation"

$$\text{for } 0 < x < a: \quad \psi(x) = Fe^{-k_3x} + Ge^{k_3x}$$

$$\text{with } k_3 = \frac{\sqrt{2m(V_0 - E)}}{\hbar}$$

Completing the solution requires imposing conservation of  $\psi(x)$  and  $\psi'(x)$  that leads to link  $A, B, C, F$  (note:  $D = 0$  since there is no reflection from the right)



Approximate expression of the transmission coefficient  $T$ , i.e., **probability for the particle to cross the barrier**

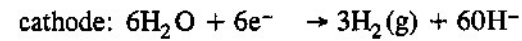
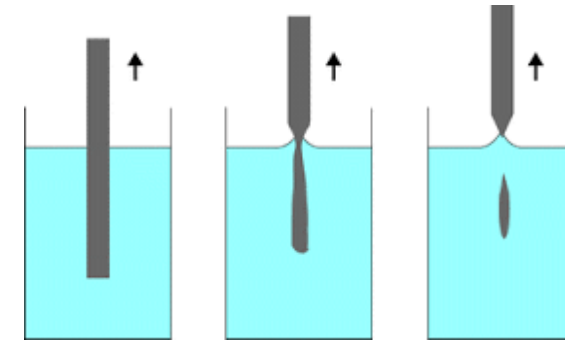
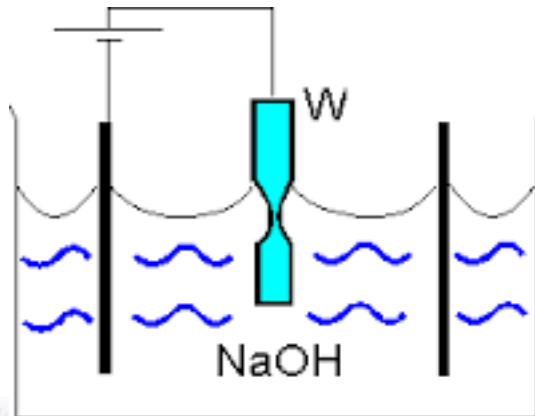
**The transmission coefficient depends exponentially on the barrier length  $a$**

$$T \approx 16 \frac{E}{V_0} \left( 1 - \frac{E}{V_0} \right) e^{-2ka}$$

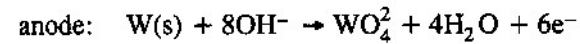
$$\text{with } ka = \frac{\sqrt{2mV_0a^2 \left( 1 - \frac{E}{V_0} \right)}}{\hbar}$$

# STM PROBES

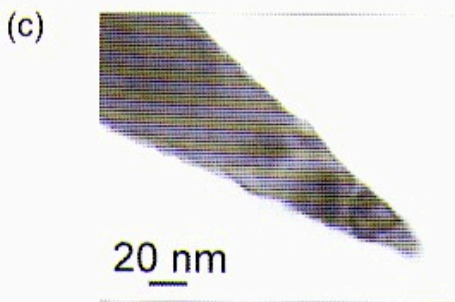
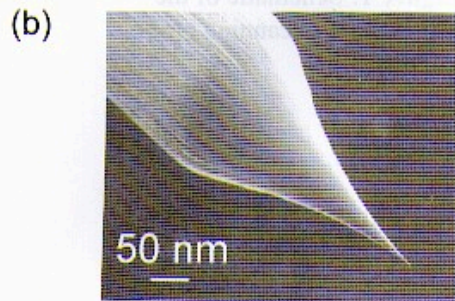
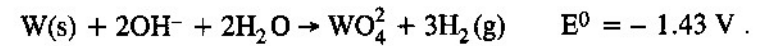
Electrochemical etching of W (or Pt/Ir) is typically used



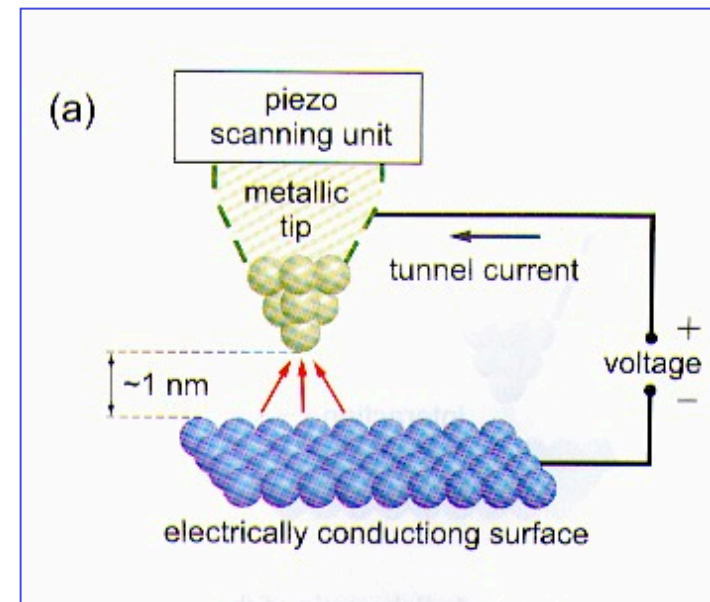
SRP = - 2.45 V



SOP = + 1.05 V



**Very sharp tips can be obtained (ideally, terminated by a "single" atom)**



# OPERATING MODES

The tunneling current depends exponentially on the distance, i.e., on the barrier width

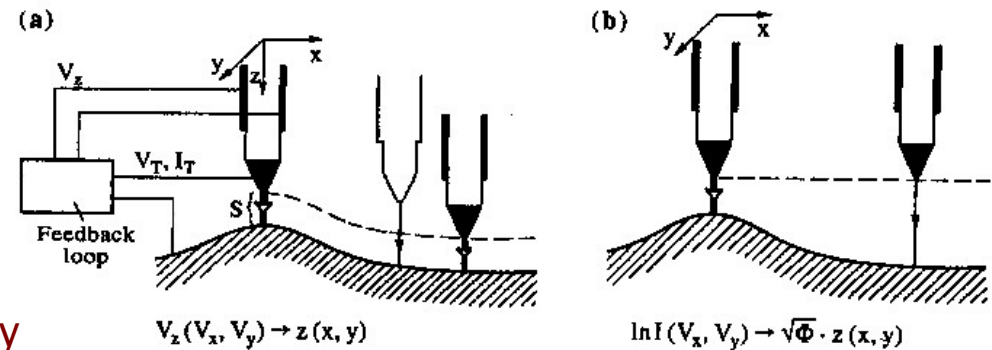
## Constant height:

The current is measured and mapped

## Constant gap;

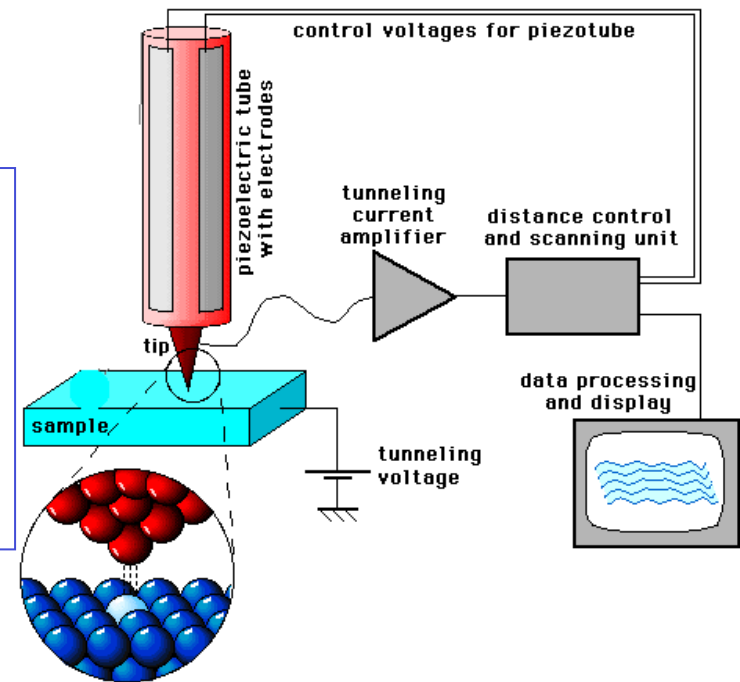
A *feedback circuit* keeps the current constant by acting on the tip-to-sample distance

The “error signal”, i.e., the signal sent to the translator, is mapped, being representative of the **local topography**



## STM:

- ✓ Probe is a conductive tip
- ✓ Sample (surface) is conductive or semiconductive
- ✓ A bias voltage is applied between sample and tip
- ✓ Tip is kept at small distance from the surface (typ < 1 nm)
- ✓ Tunneling current (typ in the pA range) is measured and eventually used for the feedback



# MORE ON TUNNELING

## Tunneling Effect in Quasiclassical Approximation

The quasiclassical qualitative condition imply that de Broglie wavelength of the particle  $\lambda$  is less than characteristic length  $L$  determining the conditions of the problem. This condition means that the particle wavelength should not change considerably within the length of the wavelength order

$$\left| \frac{d\tilde{\lambda}}{dz} \right| \ll 1 \quad (1)$$

where  $\tilde{\lambda} = \lambda / 2\pi$ ,  $\lambda(z) = 2\pi\hbar / p(z)$  – de Broglie wavelength of the particle expressed by way of the particle classical momentum  $p(z)$  [1].

Condition (1) can be expressed in another form taking into account that

$$\frac{dp}{dz} = \frac{d}{dz} \sqrt{2m(W - U)} = -\frac{m}{p} \frac{dU}{dz} = \frac{mF}{p} \quad (2)$$

where  $F = -dU/dz$  means classical force acting upon the particle in the external field. Introducing this force, we get

$$\frac{m\hbar|F|}{p^3} \ll 1 \quad (3)$$

From (3) it is clear that the quasiclassical approximation is not valid at too small momentum of the particle. In particular, it is deliberately invalid near positions in which the particle, according to classical mechanics, should stop, then start moving in the opposite direction. These points are the so called "turning points". Their coordinates  $z_1$  and  $z_2$  are determined from the condition  $E=U(z)$ . It should be emphasized that condition (3) itself can be insufficient for the permissibility of the quasiclassical approach. One more condition should be met: the barrier height should not change much over the length  $L$ .

Let us consider the particles move in the field shown in Fig. 1 which is characterized by the presence of the potential barrier with potential energy  $U(z)$  exceeding particle total energy  $E$  and meeting all the quasiclassics conditions. In this case points  $z_1$  and  $z_2$  are the turning points.

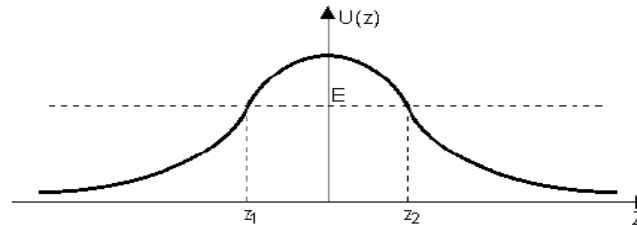


Fig. 1. Potential barrier of arbitrary shape

The approximation technique of the Schrodinger equation solution when quasiclassical conditions are met was first used by Wentzel, Kramers and Brillouin. This technique is known as WKB approximation or quasiclassical quantization method. In this textbook we do not present the Schrodinger equations solution for the given case. However, it can be found in [1], [2] and the barrier transparency in this case is

$$D(E) \propto \exp \left\{ -\frac{2}{\hbar} \int_{z_1}^{z_2} \sqrt{2m(U(z) - E)} dz \right\} \quad (4)$$

Comparing expressions (3) in chapter **Tunneling Effect** for transmission coefficients of rectangular barrier (precise solution of Shrodinger equation) and (4) for quasiclassical approximation, we can notice that there is no qualitative difference between them. In both cases the transparency decreases exponentially with the barrier width.

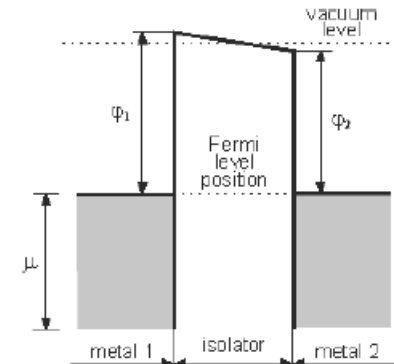


Fig. 1. Diagram of MIM system in equilibrium.  $j_1$  and  $j_2$  – work function of the left and right metals, respectively

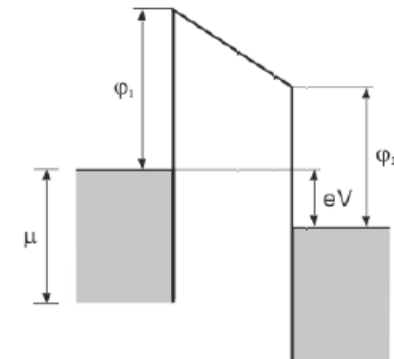


Fig. 2. Model of MIM system then positive potential is applied to the right metal

The actual shape of the barrier depends on the presence of the voltage bias, needed in turn to collect the current

Semiclassical approach leads to an approximate solution, also featuring an exponential behavior

# DEPENDENCE ON BIAS AND ON MATERIAL

The bias modifies the energy of the electron, hence the tunneling current

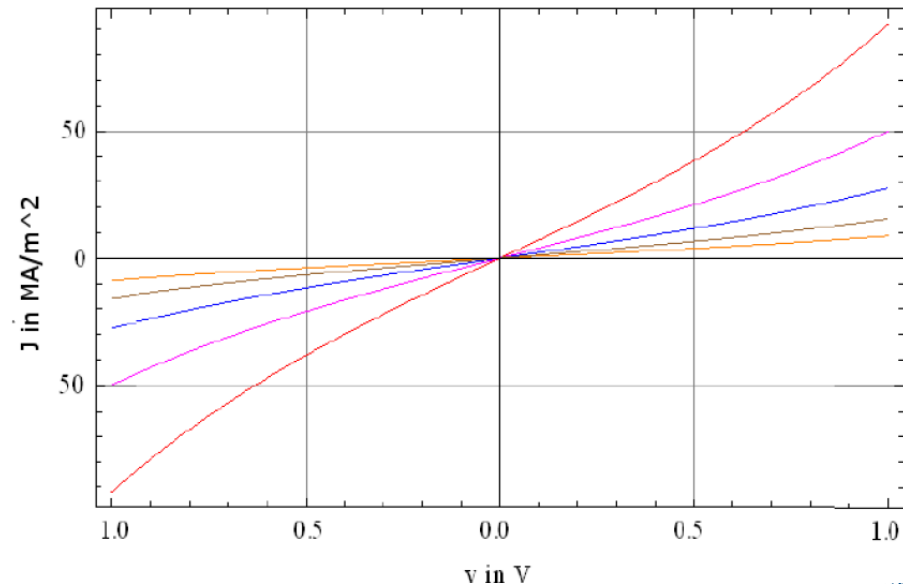
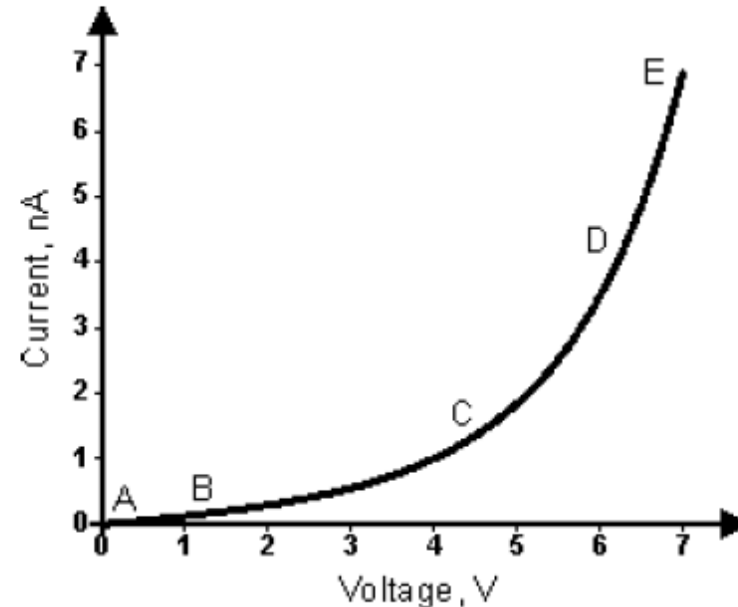
The actual dependence accounts for the occurrence of different regimes ranging through an almost-linear to an almost exponential behavior corresponding to tunneling in different conditions

Typically, bias voltage on the order of a fraction of  $V$  is used

The material affects the tunneling current mainly through the **workfunction**

At increasing workfunction, i.e., increasing extraction voltage, the tunneling current decreases (and the tunneling behavior may change as a function of the bias voltage)

$$J = \frac{\gamma \sqrt{\phi} V}{\delta_z} \exp(-A \delta_z \sqrt{\phi})$$



# LOCAL DENSITY OF STATES

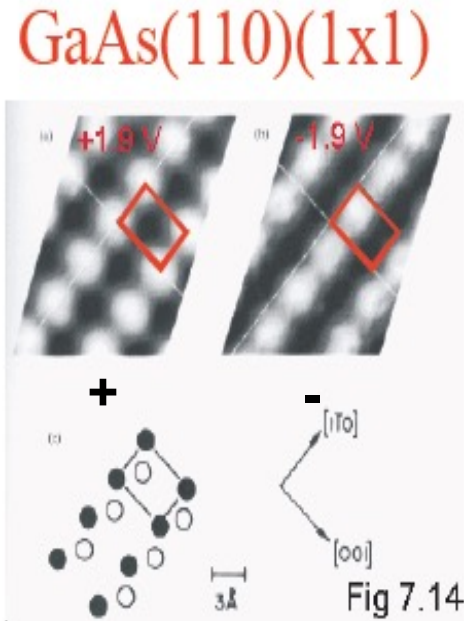
In a quantum picture, the tunneling probability depends on the density of states (actually, on the combined DOS of the tip and of the sample surface)

Local Density Of States (LDOS) can produce a modulation of the tunneling current when scanning a surface

In the constant gap mode, the feedback sense the LDOS modulation as a topography modulation

The topography reconstructed by STM is *always* the result of a kind of convolution of different effects (at least at the atomic scale)

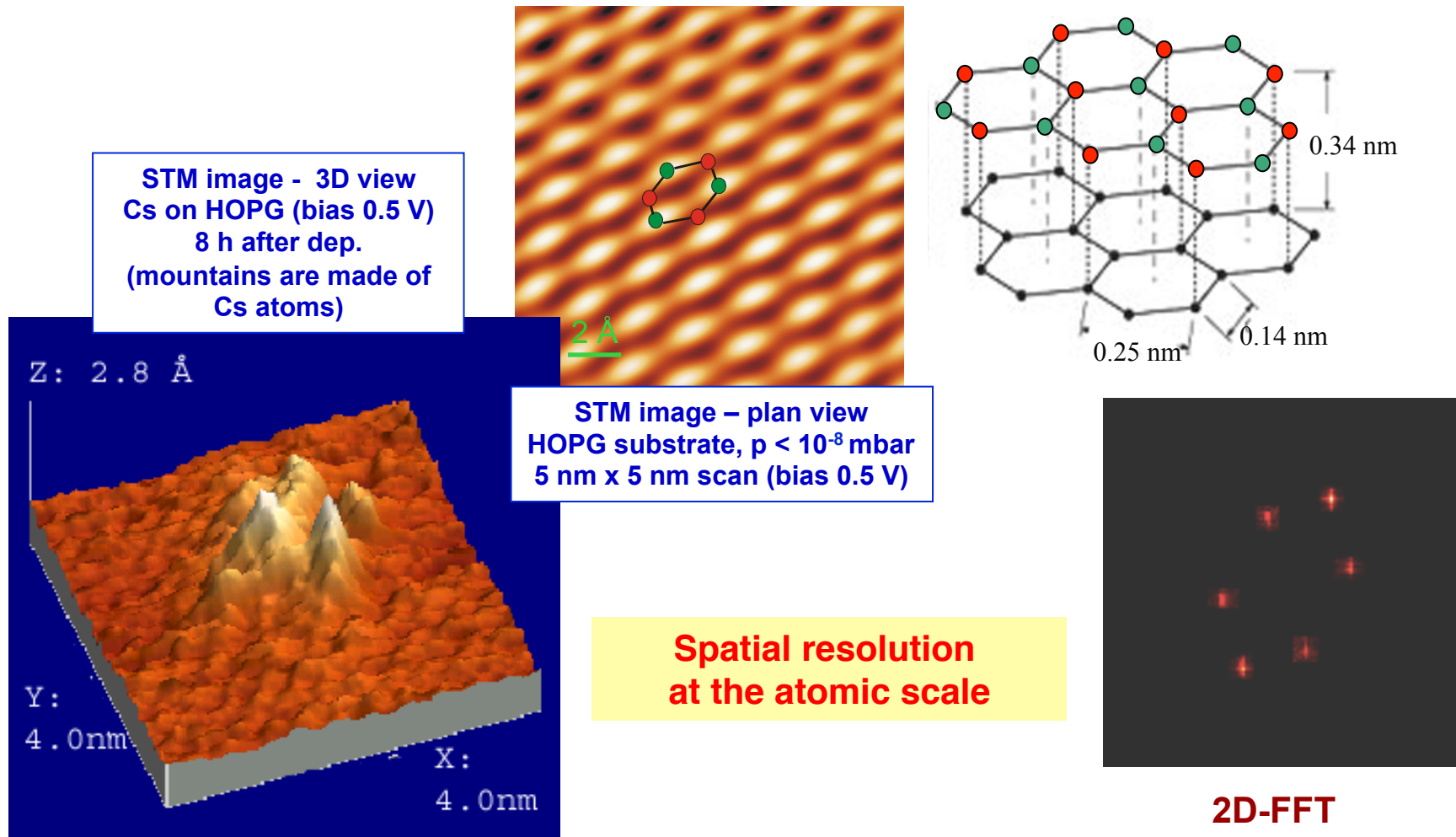
- Local density of states: the definition:  $g(\vec{r}, E) = \sum_n |\psi_n(\vec{r})|^2 \delta(E - E_n)$ 
  - LDOS is the charge density at point  $r$  resulting exclusively from states in the energy interval from  $E$  to  $E + dE$ .
  - If we sum LDOS over all atom in the system, we will get the total DOS because of the normalization condition on the wave function
  - In periodic systems without defects DOS and LDOS are equivalent



For instance, with **semiconductors** the STM image depends on the bias polarity (LDOS of the surface is different depending on the sign of the tunneling)

# EXAMPLES I

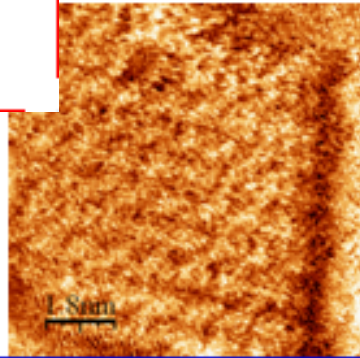
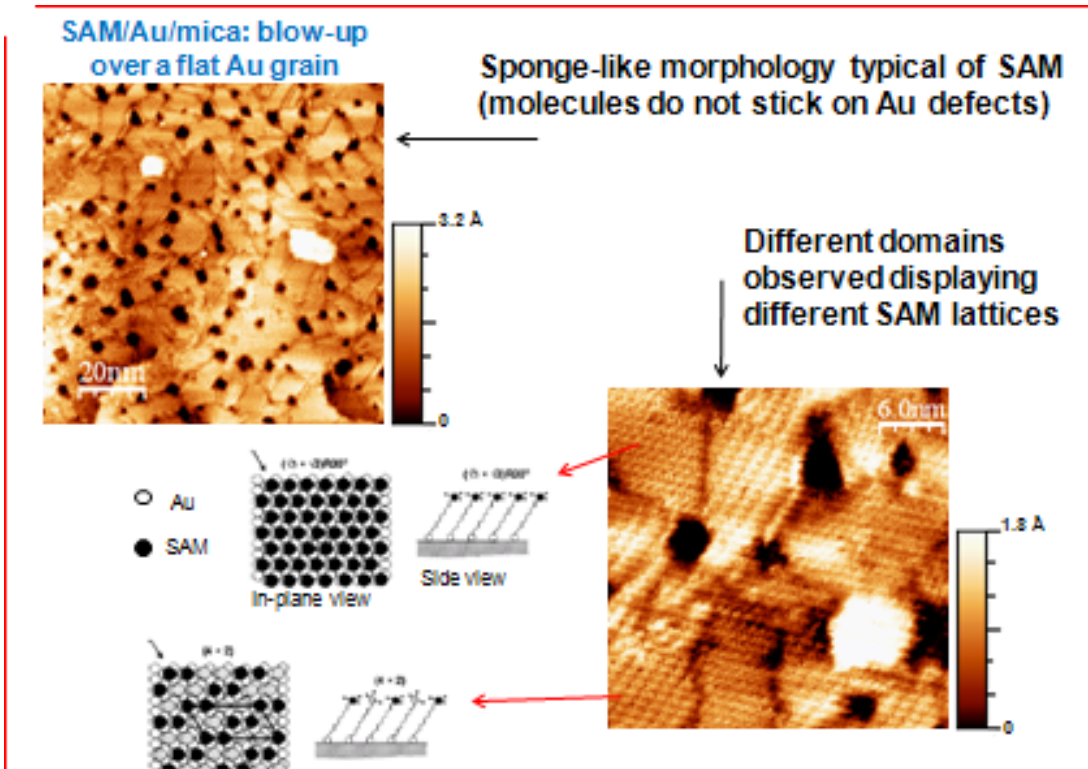
Highly Oriented Pyrolytic Graphite (HOPG) substrates well suited as test samples



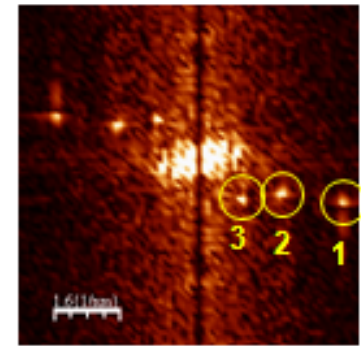


# EXAMPLES II

While having a practically dielectric character, SAM molecules deposited on Gold can be imaged thanks to inter-molecule tunneling (very thin layer, thickness ~ nm)



UHV-STM image – plan view  
SAM/Au/mica substrate  
estimated surface coverage  $\theta < 0.05$



Three regular structures detected  
Possible explanation (to be further assessed):

1. Au ( $\sqrt{3} \times \sqrt{3}$ ), step ~ 0.29 nm
2. SAM ( $\sqrt{3} \times \sqrt{3}$ )R30°, step ~ 0.50 nm
3. Cs ( $\sqrt{3} \times \sqrt{3}$ ), step ~ 0.85 nm

**Regular SAM coating well detected by STM thanks to its excellent spatial resolution**

## EXAMPLES III

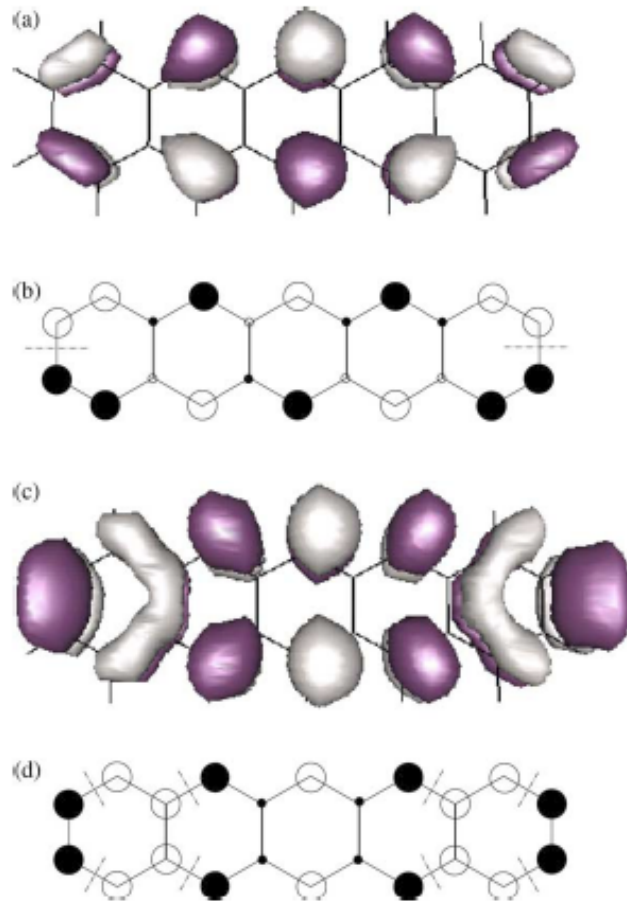
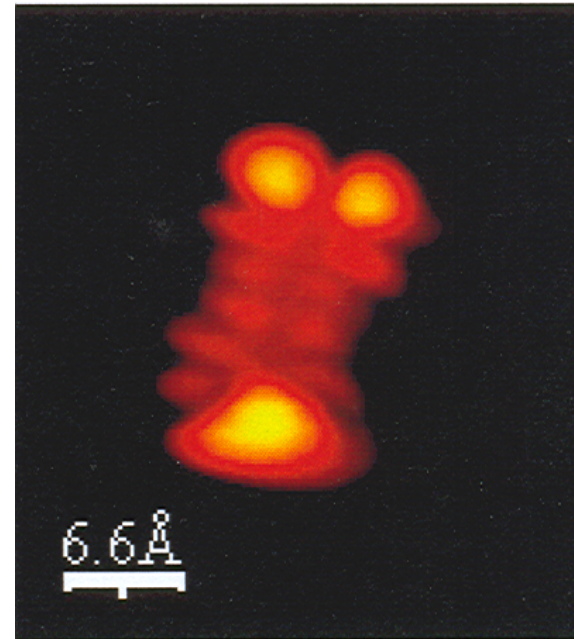


Fig. 2. Single particle wavefunctions of isolated pentacene molecule. The dark color represents a positive sign, the light color a negative sign. (a) and (b) show the HOMO, (c) and (d) the LUMO. (a) isosurface at  $\pm 0.05/\text{\AA}^3/2$ ; (b) LCAO coefficients: small circles 0.01–0.09, large circles 0.12–0.3, the short lines show regions of high gradients; (c) isosurface at  $\pm 0.03/\text{\AA}^3/2$ , (d) similar to (b). Wavefunctions plotted with the program gOpenMol [28].

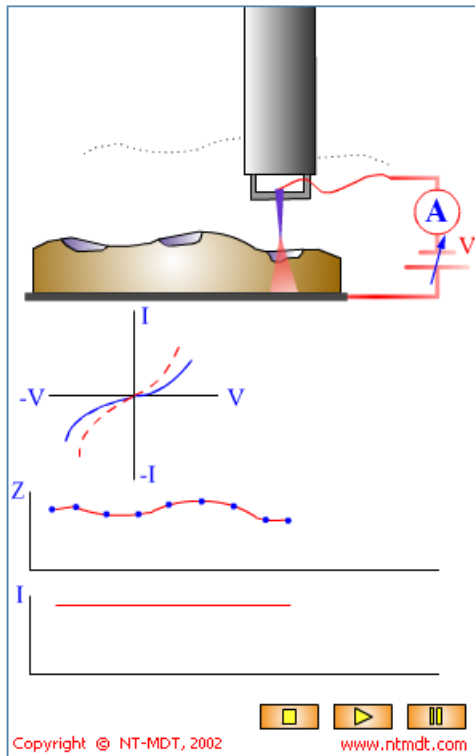


A single pentacene molecule deposited on Si

**Imaging the local density of states enables imaging “molecular orbitals”**

# STM SPECTROSCOPY

## I(V) Spectroscopy.



In I(V) Spectroscopy (or Current Imaging Tunneling Spectroscopy, CITS) a normal topographic image is acquired at fixed  $I_0$  and  $V_0$ . At each point in the image feedback loop is interrupted and the bias voltage is set to a series of voltages  $V_i$  and the tunneling current  $I_i$  is recorded. The voltage is then returned to  $V_0$  and the feedback loop is turned back on. Each I-V spectra can be acquired in a few milliseconds so there is no appreciable drift in the tip position. This procedure generates a complete current image  $I_i(x,y)$  at each voltage  $V_i$  in addition to the topographic image  $z(x,y)|_{V_0}$ .

CITS data can be used to calculate a current difference image

$D[V_i, V_j](x,y)$  where  $V_i$  and  $V_j$  bracket a particular surface state, producing an atomic resolved, real space image of a surface state. This technique, for example can be used in UHV to image filled ad-atom states or the dangling bond states for silicon reconstructions.

### References

1. G. Binnig and H. Rohrer: Surf. Sci. 126 (1983) 236. Rep. Prog. Phys. 55, 1165-1240 (1992).

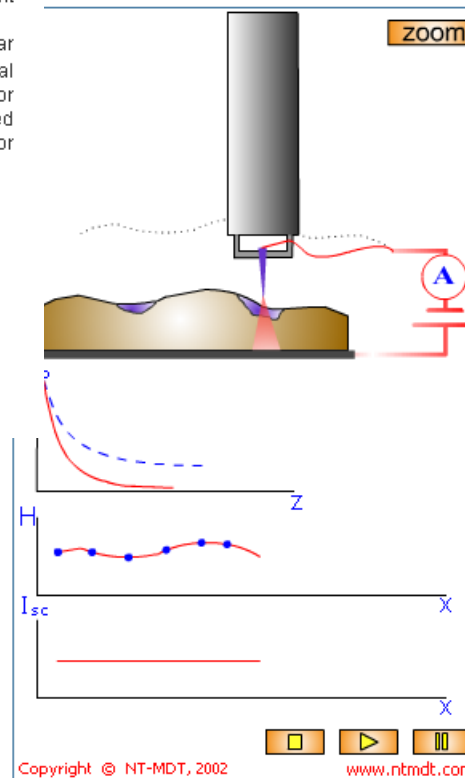
Download Flash model

Copyright © NT-MDT, 2002

www.ntmdt.com

At one point over the surface,  $I$  vs  $V$  and  $I$  vs  $Z$  curves can be acquired

## I(z) Spectroscopy.



The I(z) Spectroscopy is related to LBH spectroscopy and can be used for providing an information about the z-dependence of the microscopic work function of the surface. Next important use of the I(z) Spectroscopy is concerned with for testing of the STM tip quality.

The tunneling current  $I_T$  in STM exponentially decays with the tip-sample separation  $z$  as

$$I_T \sim \exp(-2kz),$$

where the decay constant is given by

$$2k = 2(2mU/h^2)^{1/2}$$

$U$  is the average work function  $U_{av} = (U_s + U_t)/2$ , where  $U_t$  and  $U_s$  are the tip and sample work functions, respectively.

In the I(z) Spectroscopy, we measure the tunnel current versus tip-sample separation at each pixel of an STM image. For  $U_{av} = 1$  eV  $2k = 1.025 \text{ \AA}^{-1} \text{ eV}^{-1}$ .

Sharp I(z) dependence helps in determining of tip quality. As is empirically established if tunnel current  $I_T$  drop to one-half with  $Z < 3 \text{ \AA}$  the tip is considered to be very good, if with  $Z < 10 \text{ \AA}$ , then using this tip it is possible to have an atomic resolution on HOPG. If this takes place with  $Z > 20 \text{ \AA}$  this tip should not be used and must be replaced.

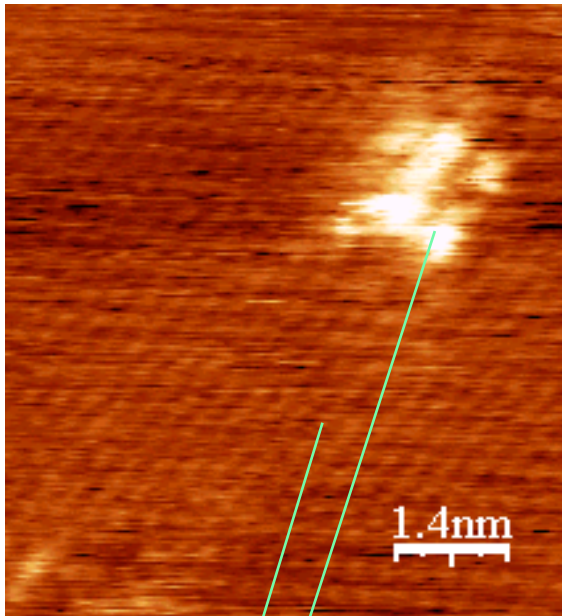
### References

Copyright © NT-MDT, 2002

www.ntmdt.com

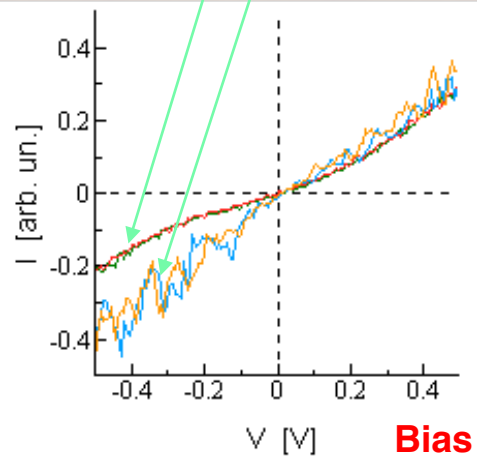
## EXAMPLES IV

I-V curves can be acquired at different positions



STM image -  
plan view  
Cs on HOPG  
(bias 0.5 V)  
8 h after dep.

Tunneling  
current  
(conversion  
factor  $10^8$ )



Typical STM I-V  
curves of different  
regions (covered/  
uncovered)

Possibility to discriminate  
“conductivity” of small-sized  
nanostructures with excellent  
space resolution and sensitivity

# EXAMPLES V

In semiconductors:  
I-V STM spectroscopy enables LDOS detection  
(and even local energy levels)

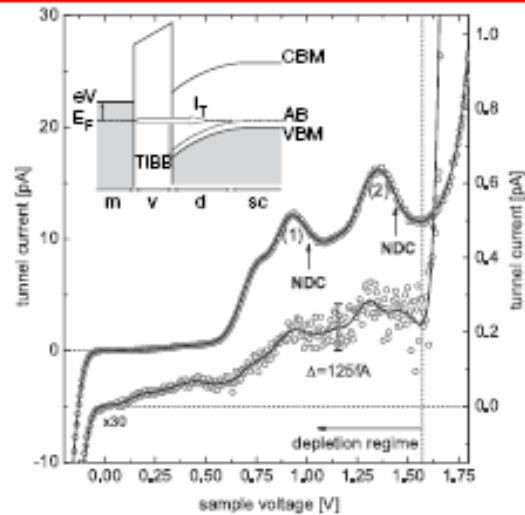
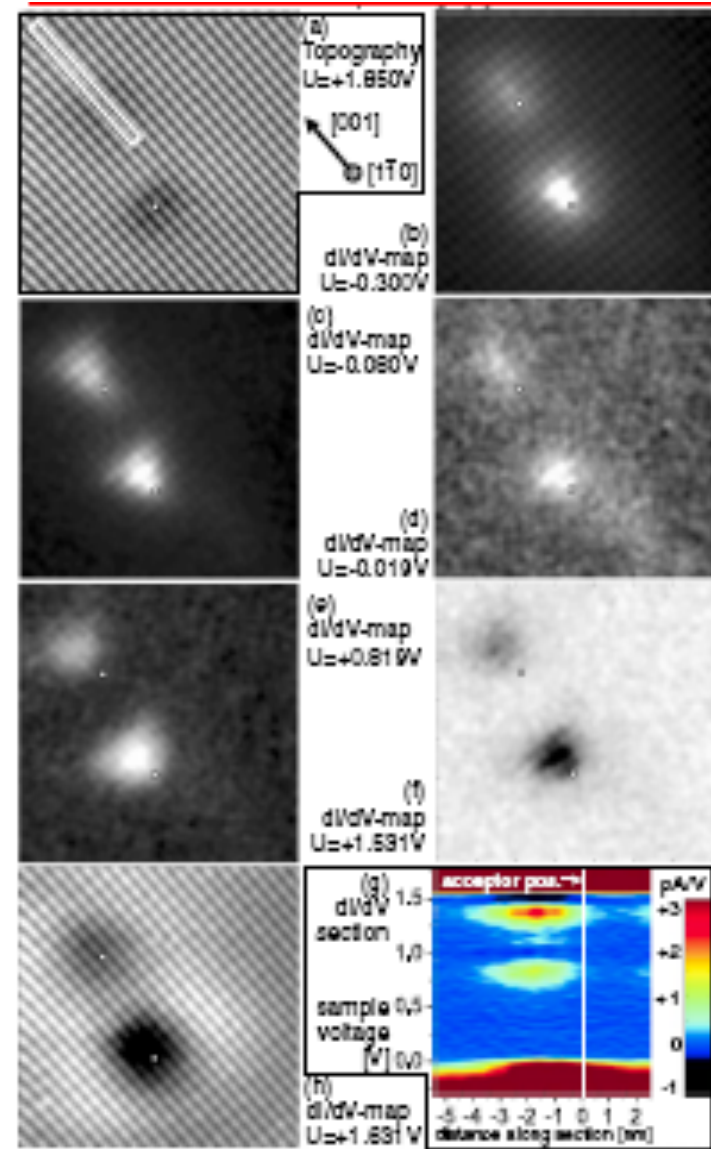


FIG. 2.  $I(V)$  characteristics of a buried carbon acceptor (upper curve) and the undisturbed surface (lower curve) obtained by spatially resolved  $I(V)$  spectroscopy (STS). The raw data are plotted as points, averaged data as lines. The  $I(V)$  curve taken on the undisturbed surface is scaled by a factor of 30 with respect to the one taken on the C acceptor. Note that the spectroscopic features indexed with (1) and (2) are followed by negative differential conductivity (NDC). Noise level for both curves is smaller than 125 fA. The inset sketches the energetic conditions of the depletion layer regime in the voltage interval from 0 V to 1.57 V in a rigid-band model: (m) metallic tip, (v) vacuum barrier, (d) depletion layer, (sc) bulk semiconductor, (TIBB) depletion barrier height, (VBM) valence band maximum, (CBM) conduction band minimum, (AB) acceptor band, and ( $I_T$ ) tunneling channel.



# VARIANTS AND CHILDS



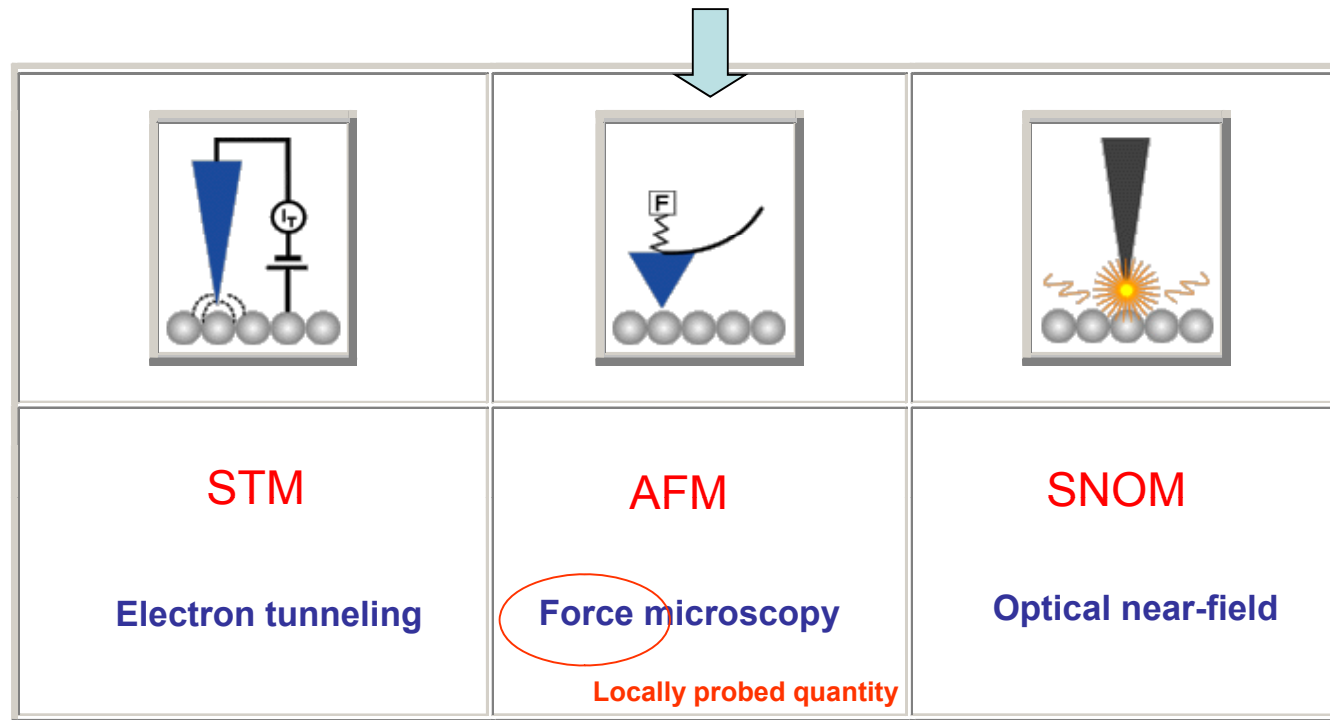
- STM is an extremely powerful microscopy technique, allowing sub-nm spatial resolution accompanied with measurements of a physical quantity (tunneling current) which can represent local variations of different material properties (workfunction, conductivity, LDOS in general)
- Once the appropriate meaning is given to *topography* (not well defined at the atomic scale!), the feedback mechanism and the possibility to operate with *calibrated and reliable* piezoscanners enable **true reconstruction** of the topography, not possible with SEM/TEM



- STM is however **limited in applicability**: samples must allow for tunneling to take place (i.e., it must be either a conductive/semiconductive material, or a very thin dielectric layer)
- Furthermore, the measured quantity turns to depend on different material parameters, quite often in a complicated fashion (hard to be modeled)

**The technology (piezoscanner, probes, electronics) and the concepts (feedback) behind STM have been soon translated into a variety of SPM techniques in order to extend the applicability (*and to measure different material properties*)**

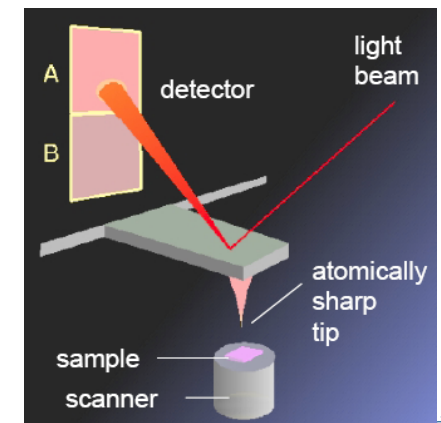
# ATOMIC FORCE MICROSCOPY



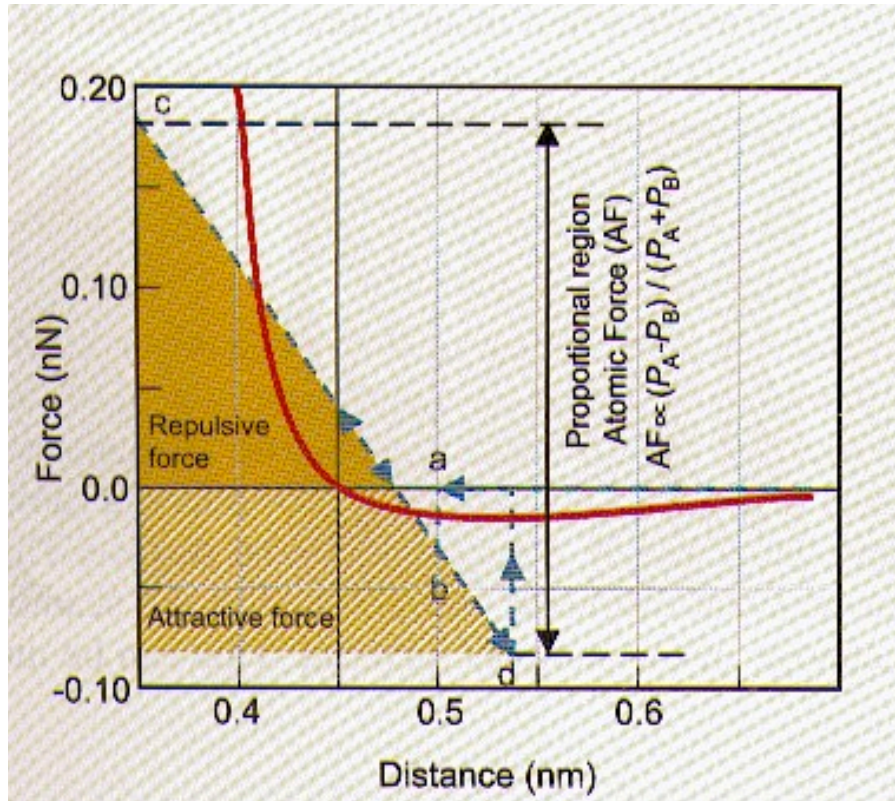
*AFM is probably the most straightforward (and easy to understand/interpret) probe microscopy*

Since the probed quantity is the mechanical interaction, AFM can be applied to virtually any class of materials (no need for specific electrical or optical properties)

*Force is sensed by a kind of transducer that translates the force into a displacement, to be measured*



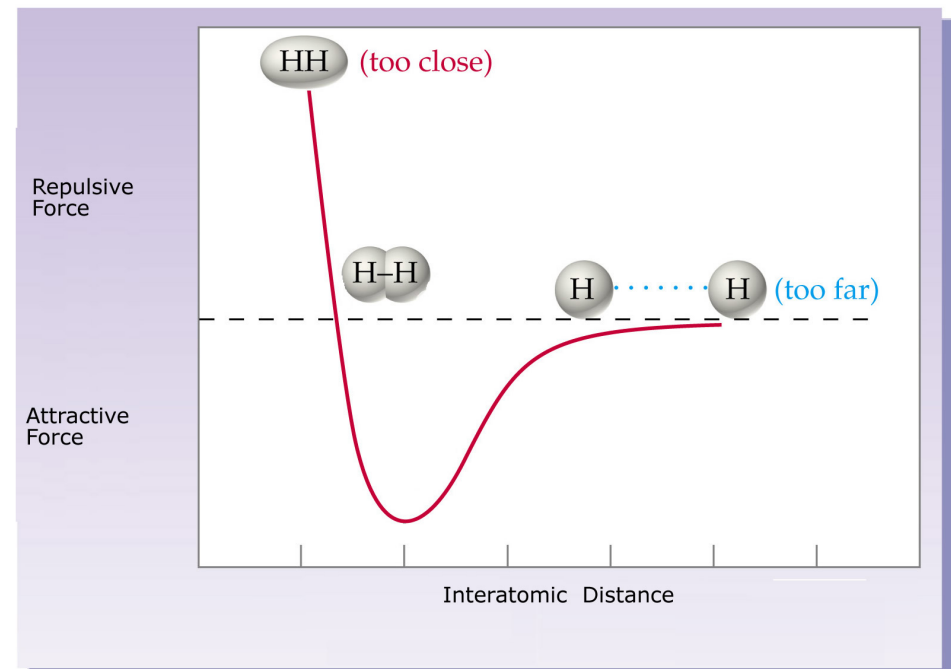
# FORCES AT A SURFACE



When approaching a surface, there is an initial weakly attractive force, followed by a steep change in slope leading to strongly repulsive behavior

The force can be effectively sensed by approaching a nanosized tip to the surface

The **force vs distance** behavior is typical of many phenomena and systems, e.g., molecular systems (but also stable planet-satellite systems, Yukawa potential, partly van der Waals, etc.)

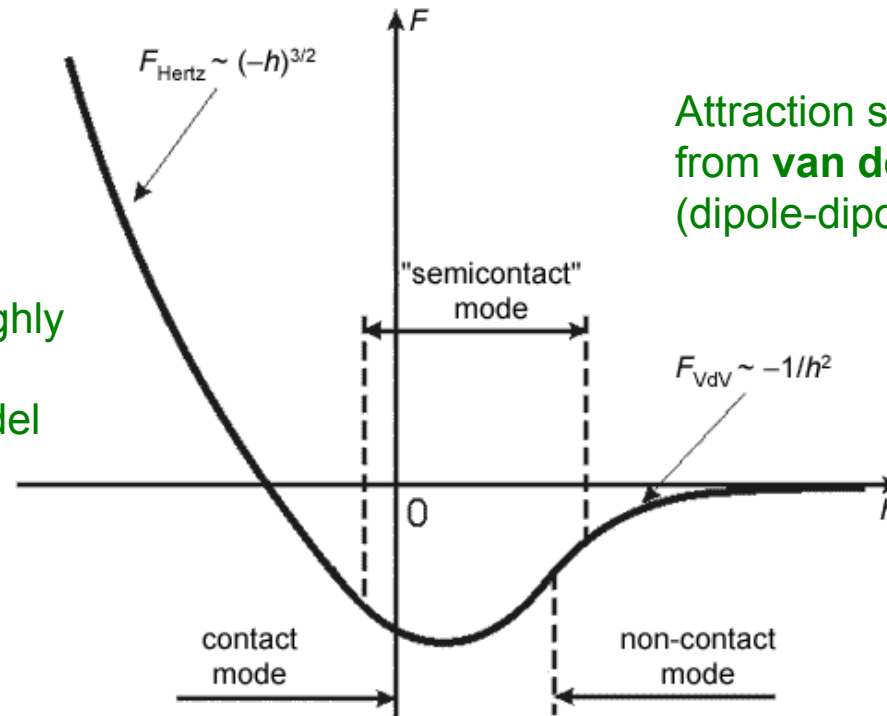




# ATTRACTION/CONTACT/REPULSION

Neglecting other processes, e.g., **adhesion, plastic deformation, etc.**

Repulsion can be roughly modeled using the continuum elastic model (**Hertz**)



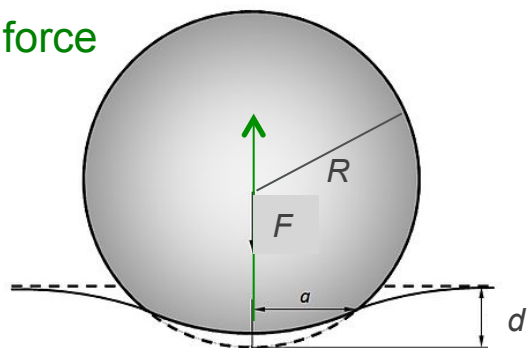
Attraction stems mostly from **van der Waals** forces (dipole-dipole).

At the atomic scale, **contact** cannot be precisely described (it is just what is in between attraction and repulsion...)

## A FEW DETAILS

A very rough picture, leading to approximate behaviors, can be drawn based on conventional models

Repulsive force



Hertzian contact between a (nano)sphere and a **flat** surface

$$F \propto d^{3/2} R^{1/2}$$

(the proportionality factor depends on both Young and Poisson coefficients)

**Dipole-dipole** (van der Waals) interactions

Note: both dipoles have an “instantaneous” character

$$U = -\vec{p} \cdot \vec{E} \quad \text{with} \quad \vec{E} = \vec{E}_{dip} = \frac{(3(\vec{p} \cdot \vec{r})\vec{r} - r^2\vec{p})}{r^5} \propto r^{-3}$$

Possible mechanisms:

- Dipole orientation
  - Dipole induction
  - Dipole displacement
- }  $\vec{p} \propto \vec{E} \rightarrow U \propto r^{-3}r^{-3} = r^{-6}$

Attractive force

$$\vec{F} = -\vec{\nabla} U \propto -r^{-s}$$

With  $s$  depending on the actual geometry, materials, size, etc.

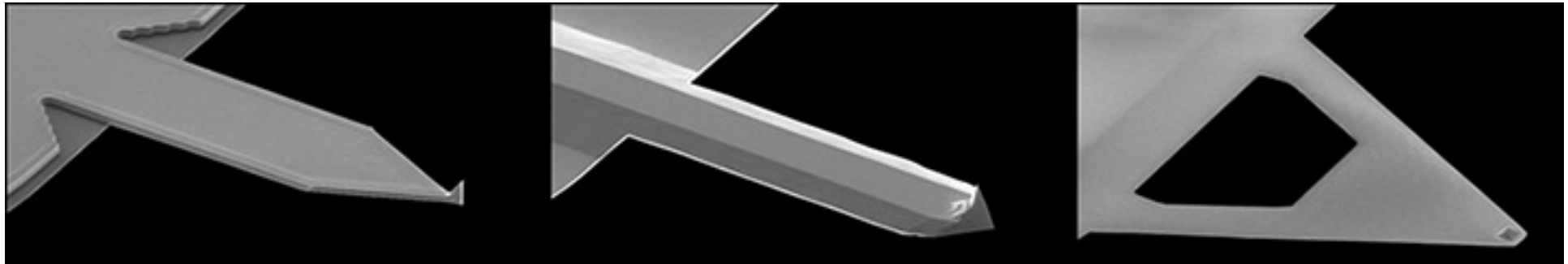
$$F \propto -d^{-2 \div -4}$$

From the point of view of the force intensity, both mechanisms lead typically to forces around  $10^{-8} - 10^{-9}$  N  
(rather weak, still measurable, as we will see)

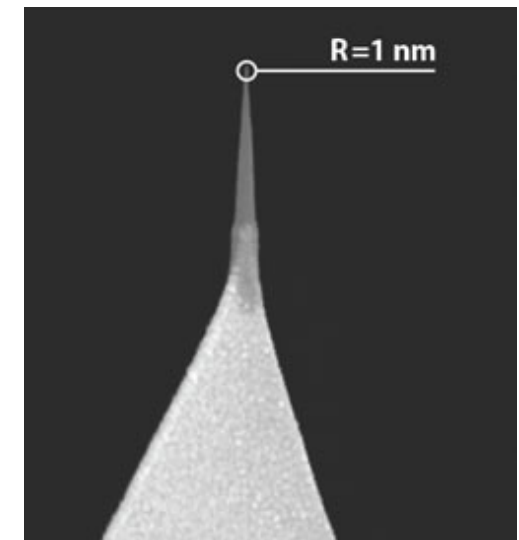
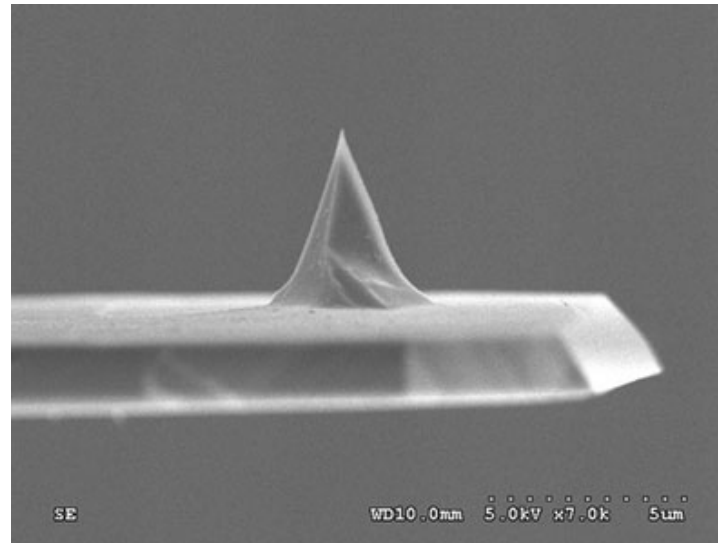
# AFM PROBES I

Reliability of AFM is strongly indebted with the availability of suitable probes, presently found in a great variety of shapes, sizes, operating parameters, materials.

Here,  $\text{Si}_3\text{N}_4$  cantilevered probes are mostly considered



Typically, a hard and sharp tip at the end of a flexible beam (cantilever)



# EXAMPLES OF FABRICATION

The first step in the fabrication of an AFM tip is the etching of a single-crystal silicon wafer with specific crystalline orientation. This results in the forming of square pyramidal tips with characteristic angles.

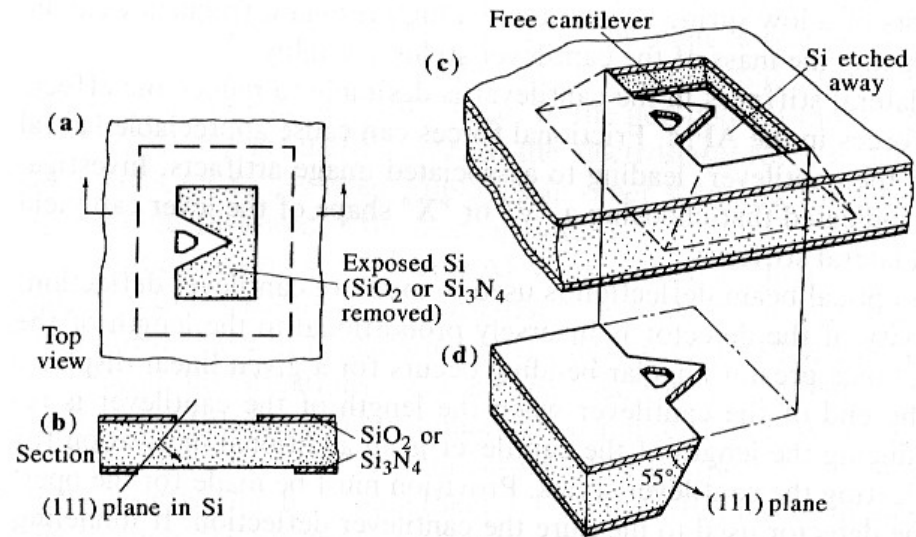
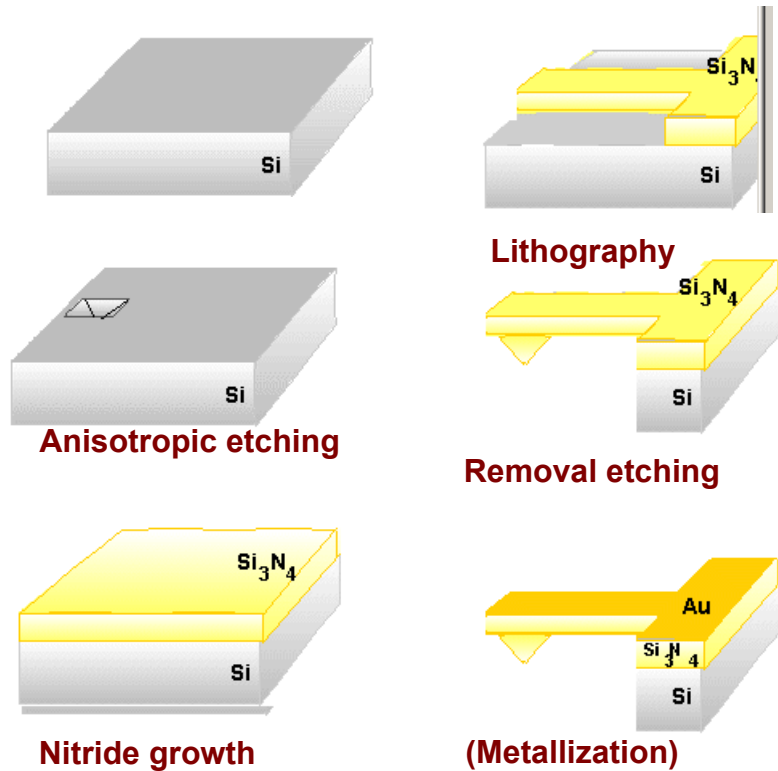
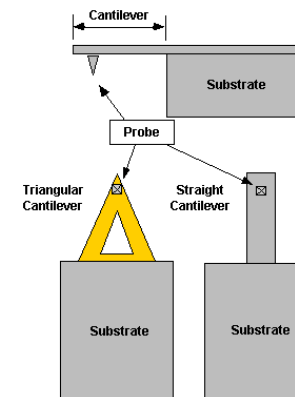
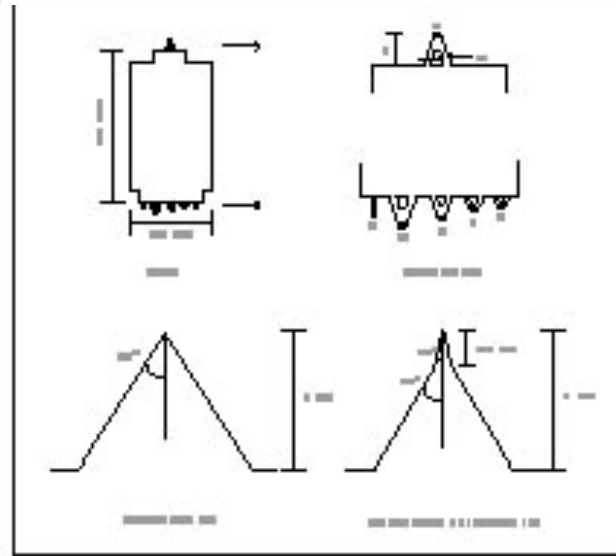


**Fig. 5.2a-d.** Fabrication of thin-film microcantilevers. (a) A thin film of  $\text{SiO}_2$  or  $\text{Si}_3\text{N}_4$  is formed on the surface of a (100) Si wafer and patterned to define the shape of the cantilever and to create openings on the top and bottom of the wafer. (b) The windows are aligned along (111) planes. (c) Anisotropic etching of the exposed Si with KOH undercuts the cantilever and self-terminates at the (111) planes as shown. (d) A small Si chip is cut from the wafer to serve as a pedestal for mounting the cantilever in the AFM [5. 4]



# AFM PROBES II



Many different cantilevers are commercially available

They are different for:

- Dimensions and shape, typ 0.1-0.5 mm:
- Elastic constant (materials and design, typ 0.05-50 N/m;
- Tip coating (conductive, super-hard, etc.)

Cantilever choice depends for instance on:

- Operation mode (contact/non contact)
- Quantities to be probed (e.g., if an electric field is needed, a conductive tip has to be used)
- Hardness and wear of the sample to be probed
- Possible material manipulation (e.g., nanoindentation requires super-hard tips)

# OPTICAL LEVER

cantilever displacement both quadrants of the photodiode (A and B) have the same irradiation  $P_A = P_B = P/2$  ( $P$  represents the total light intensity). The change of the irradiated area in the quadrants A and B is a linear function of the displacement

$$\delta \propto \Delta d = 2 \sin(\Theta) \cdot S_2 = 2\Theta \cdot S_2 = 3S_2 \cdot \delta/L \quad (10)$$

For small angles  $\sin(\Theta) \approx \Theta$  and  $\Theta$  may be evaluated from the relation  $\Theta = 3\delta/2L$  (Figure 18b). For  $P_A$  and  $P_B$  one would get approximately  $P_A = P/2 \cdot (d + \Delta d)/2$  and  $P_B = P/2 \cdot (d - \Delta d)/2$ . Using the simple difference between  $P_A$  and  $P_B$  would lead to  $\Delta P = P \cdot 3S_2 \delta / (Ld)$  but in this case one cannot distinguish between the displacement  $\delta$  of the cantilever and the variation in the laser power  $P$ . Hence the normalised difference is used, which is only dependent of  $\delta$ :

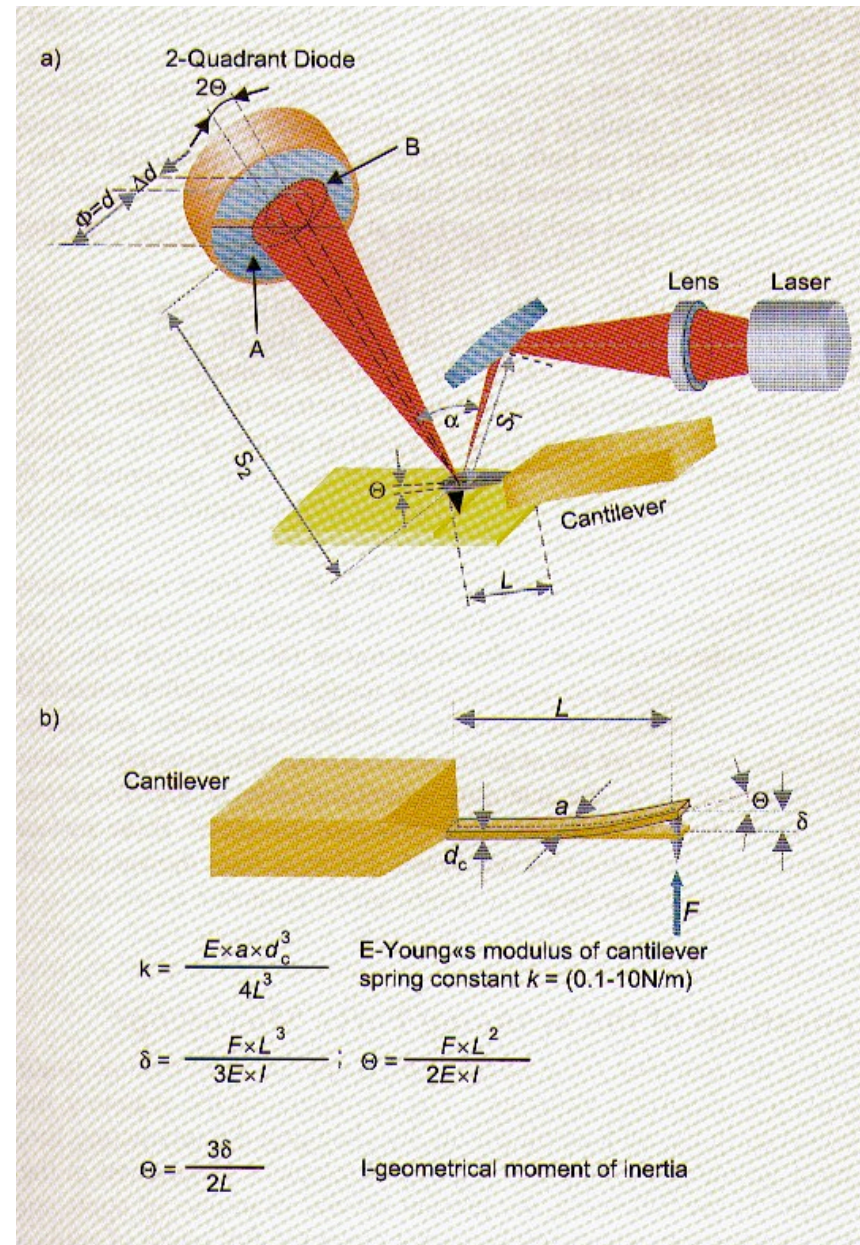
$$\frac{P_A - P_B}{P_A + P_B} = \delta \cdot \frac{3S_2}{Ld} \quad (11)$$

The "lever amplification"  $\Delta d/\delta = 3S_2/L$  is about a factor of one thousand. On the basis of this kind of technique one is able to detect changes in the position of a cantilever of the order of 0.01 nm.

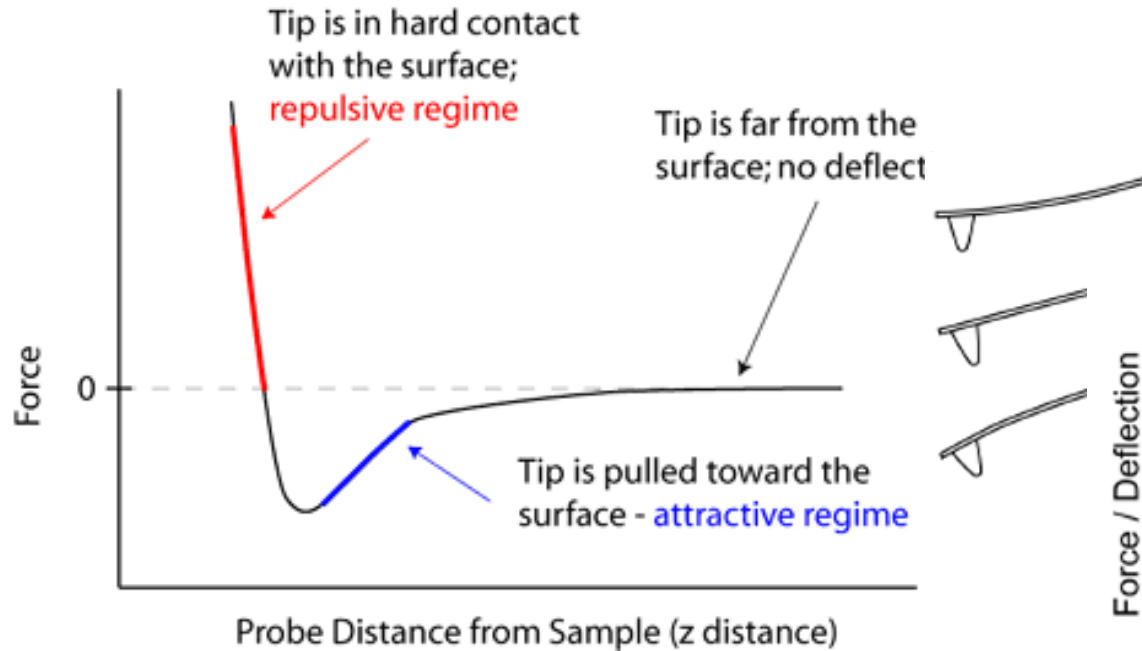
For large distances between the tip and the sample the bending of the cantilever by attractive forces is negligible. After the cantilever is brought closer to the surface of the sample (point "a" Figure 18c) the van der Waals forces induce a strong deflection of the cantilever and, simultaneously, the cantilever is moving towards the surface. This increases the forces on the cantilever, which is a kind of positive feedback and brings the cantilever to a direct contact with the sample surface (point "b"). However, when the cantilever is brought even closer in contact to the sample, it actually begins to bend in the opposite direction as a result of a repulsive interaction ("b-c"). In the range ("b-c") the position of the laser beam on both quadrants, which is proportional to the force, is a linear function of distance. On reversal this characteristic shows a hysteresis. This means that the cantilever loses contact with the surface at a distance (point "d") which is much larger than the distance on approaching the surface (point "a").

Up to now, the actual probe, i.e. the tip of the leaf spring, has not been discussed in detail. Its preparation is particularly demanding since the tip and the sensitive spring should be one piece. Moreover, the cantilever should be as small as possible. Nowadays, such scanning tips are commercially available (in contrast to the tunnelling tips, which you should prepare yourself). Figure 19 shows such a spring with tip (cantilever) made of Si. The characteristic parameters of a cantilever has been presented in Figure 18b. The spring constant  $k = Ead^3/4L^3 \sim 0.1 - 10$  N/m of the cantilever enables topographical analysis with atomic resolution.

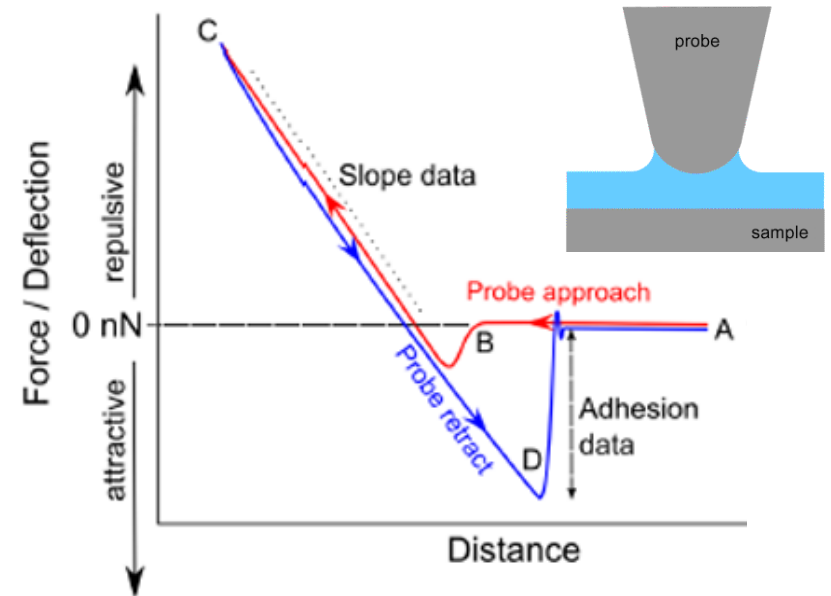
For the realisation of a scanning force microscope, the force measurement must be supplemented by a feedback control, in analogy to the scanning tunnelling microscope. The controller keeps the amplitude of the vibration of the cantilever (the tip), and thus also the distance, constant. During scanning the feedback controller retracts the sample with the scanner of a piezoelectric ceramic or shifts towards the cantilever until the vibration amplitude has reached the setpoint value again. The principle of height regulation is exactly the same as for the scanning tunnelling microscope. *The scanning force micrographs thus show areas of constant effective force constant.* If the surface is chemically homogeneous and if only van der Waals forces act on the tip, the SFM image shows the *topography of the surface*.



# FORCE VS DISTANCE CURVES



Adhesion usually takes place, as clearly seen in actual force vs distance curves



Assuming  $F \sim \text{nN}$  and  $k_{\text{cantilever}} \sim 0.1 \text{ N/m}$ , nm displacement can be read (and must be handled!)

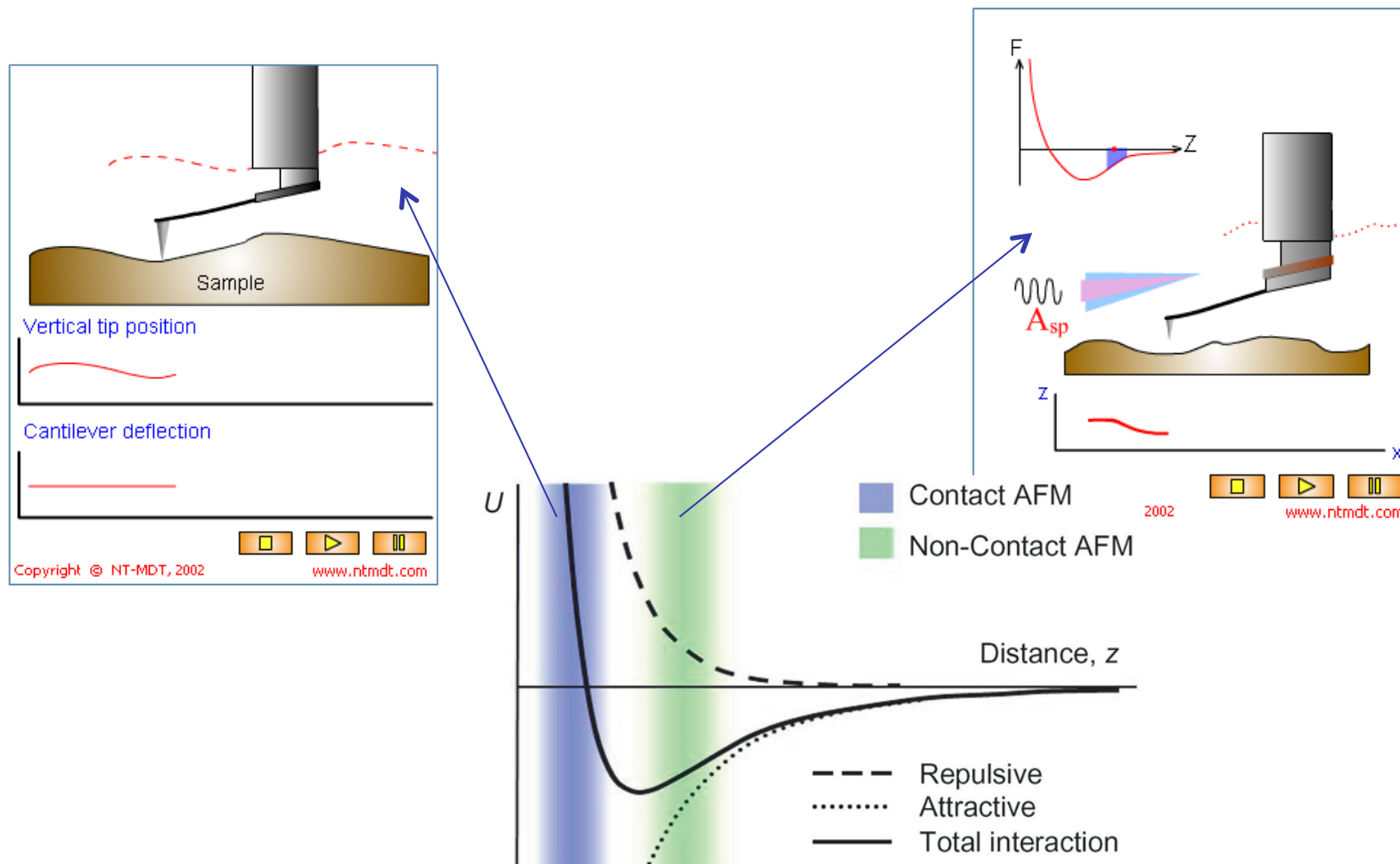
***In any case, tip/surface contact is detrimental (tip wear and/or surface scratches) and generally unwanted***

***Other “non-linear” (hysteretic) processes can occur as well, e.g., indentation***

# OPERATING MODES OF AFM

In general, a topography map is built from AFM scans using feedback like in STM

- The most used operating mode is **constant gap**, that means **constant force**
- This can be realized either **in contact** or in **intermittent contact** (aka **non contact**)



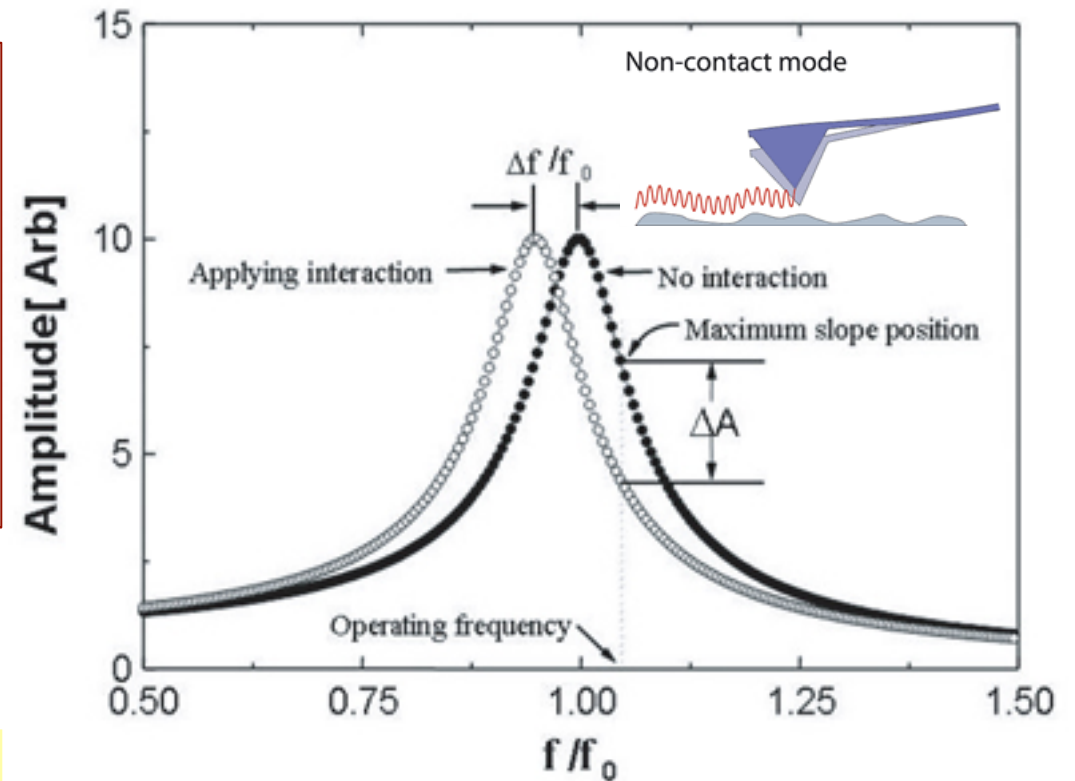


# NON-CONTACT MODE

The tip is kept in oscillation along a direction orthogonal to the surface (**tapping oscillation**)

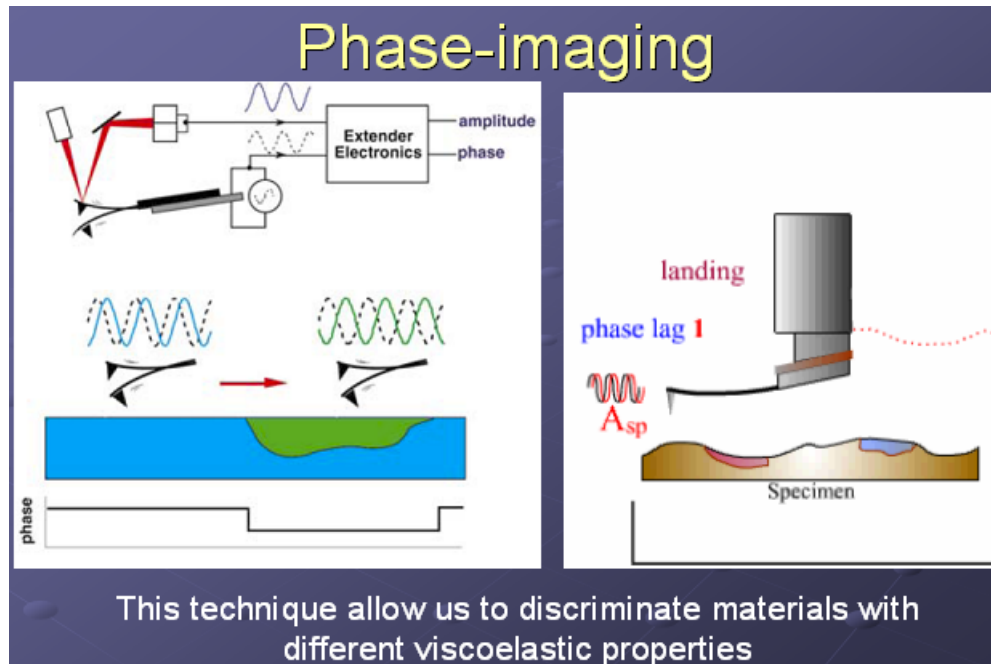
Being the cantilever an harmonic oscillator, oscillation can be driven at the resonance frequency, typically in the 100 kHz range (selectable in a wide range, as a function of the thickness and size of the cantilever)

Through the **tapping mode**, sensitive demodulation techniques can be applied leading to non-contact operation (*almost non contact*) and access to specific information (see later)



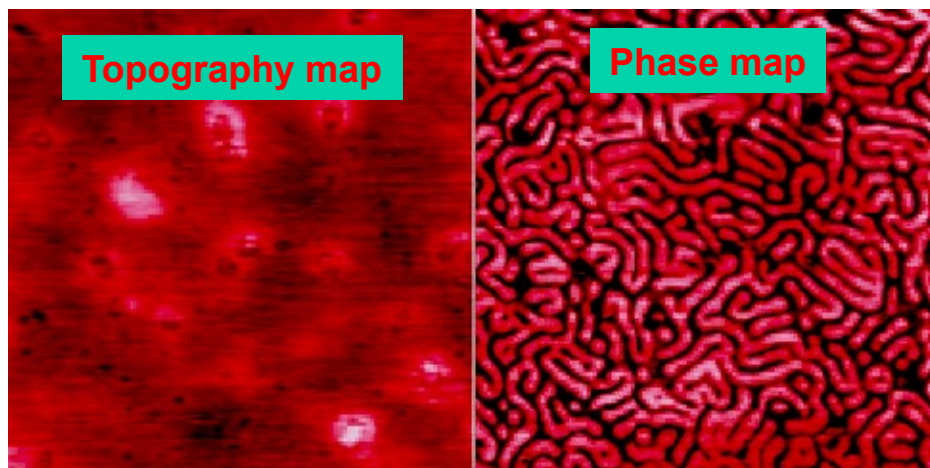
The oscillation “parameters” (frequency, amplitude, phase) are very sensitive to any kind of additional, or modified, interaction with the surface

# INTERMITTENT CONTACT



Dephasing between mechanical oscillation (e.g., the tapping oscillation) and the response of the surface (affecting the tip deflection) depends on the **viscoelasticity** of the surface (purely elastic vs Newton fluid)

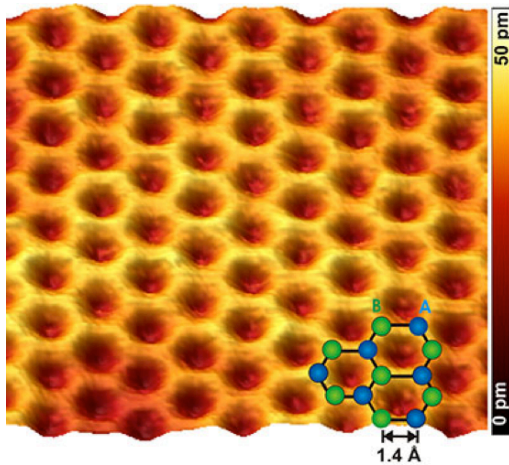
Interpretation similar to a forced and damped mechanical oscillator



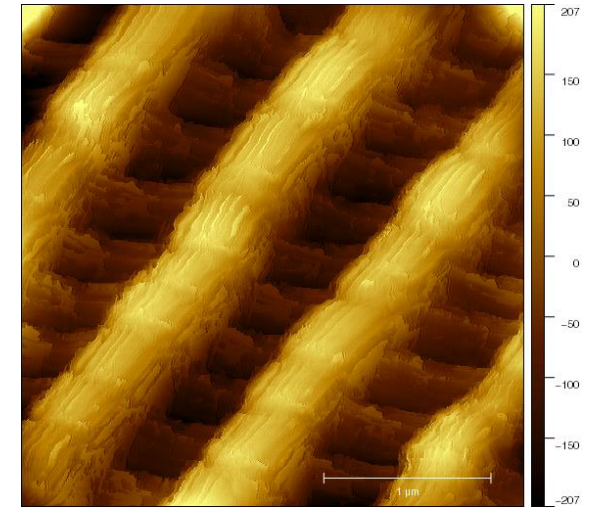
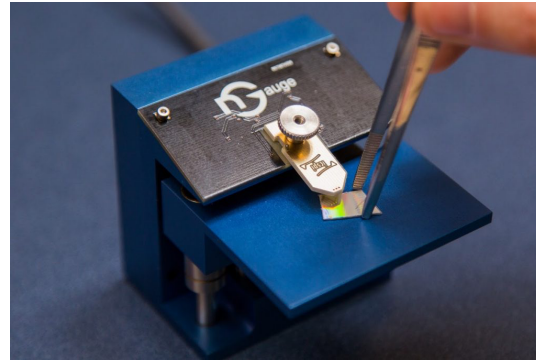
“Phase imaging”:

- adds a contrast mechanism;
- allows for local material analyses (very useful for block copolymer or other multiphasic solids)

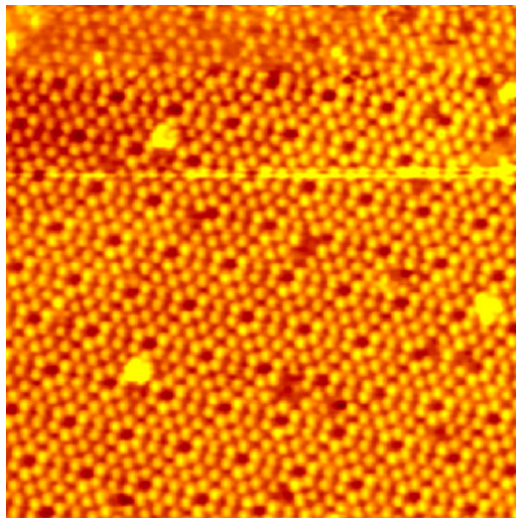
# EXAMPLES I



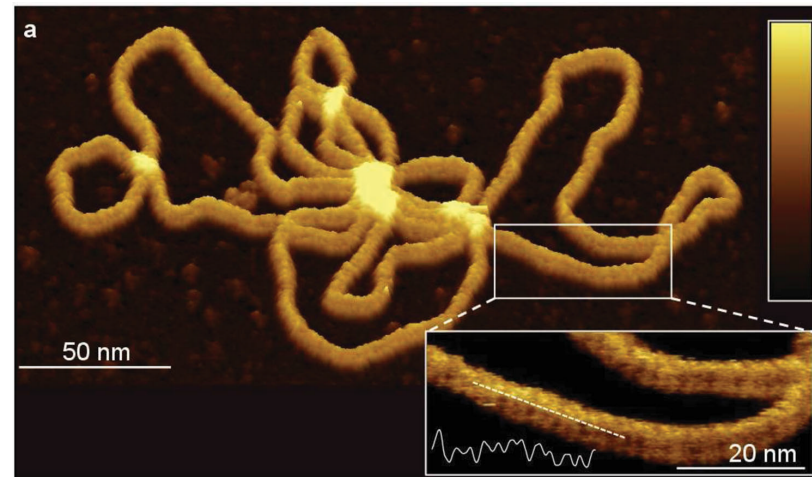
Atomic resolution on graphene



Butterfly wing

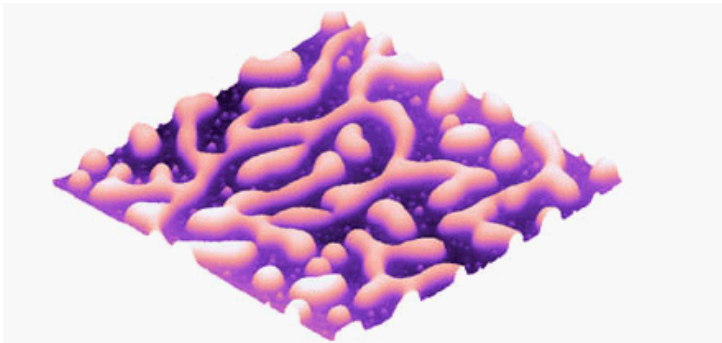


Si (111) surface

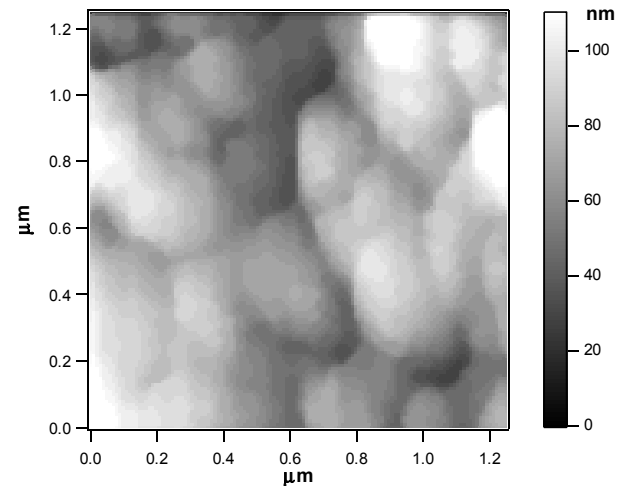


DNA plasmid adsorbed on mica  
[Pyne et al., Small (2014)]

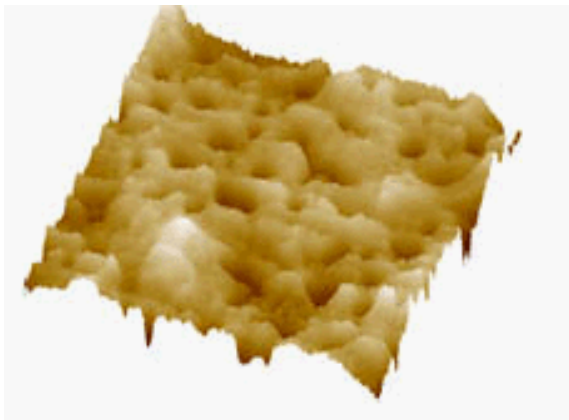
## EXAMPLES II



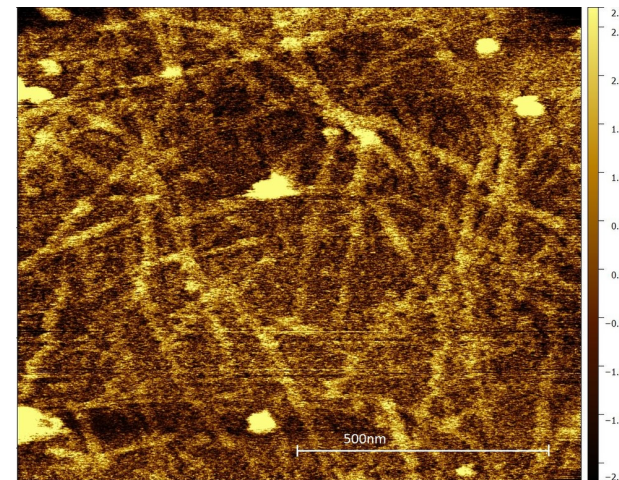
TappingMode AFM image of poly(styrene) and poly(methyl methacrylate) blend polymer film. The film was spin-cast on mica substrate from chloroform solution. The surface structure is resulted from the spinodal decomposition. The islands consist of a PMMS-rich phase while the surface matrix composes of a PS-rich phase. 3 $\mu\text{m}$  scan courtesy C. Ton-That, Robert Gordon University, U.K.



YBCO/YSZ/Ni



The sample is a strip of adhesive (3M Scotch tape) that has been peeled of a metal surface. The image shows small pits in the sticky surfaces of the adhesive. The image was acquired in TappingMode at frequency of 3 Hz and setpoint of 1.8 V. 2 $\mu\text{m}$  scan courtesy L. Scudiero, Washington State University, USA.

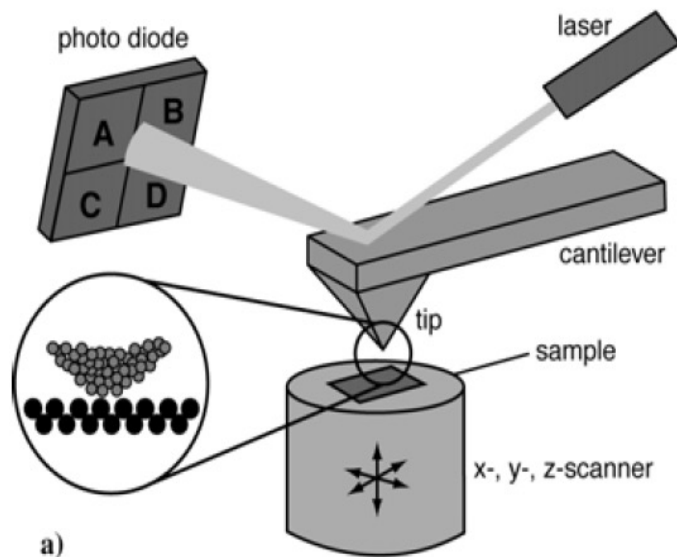


Multiwalled  
CNT on glass

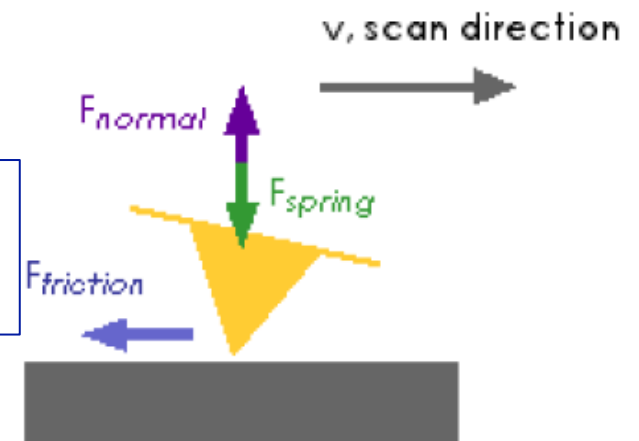
## (A FEW) VARIANTS OF AFM

The strength of AFM is also in the possibility to implement variants (often) aimed at measuring various material parameters (in addition to topography)

**Lateral forces** can be easily implemented by using a 4-quadrant detector able to measure the cantilever **twist**

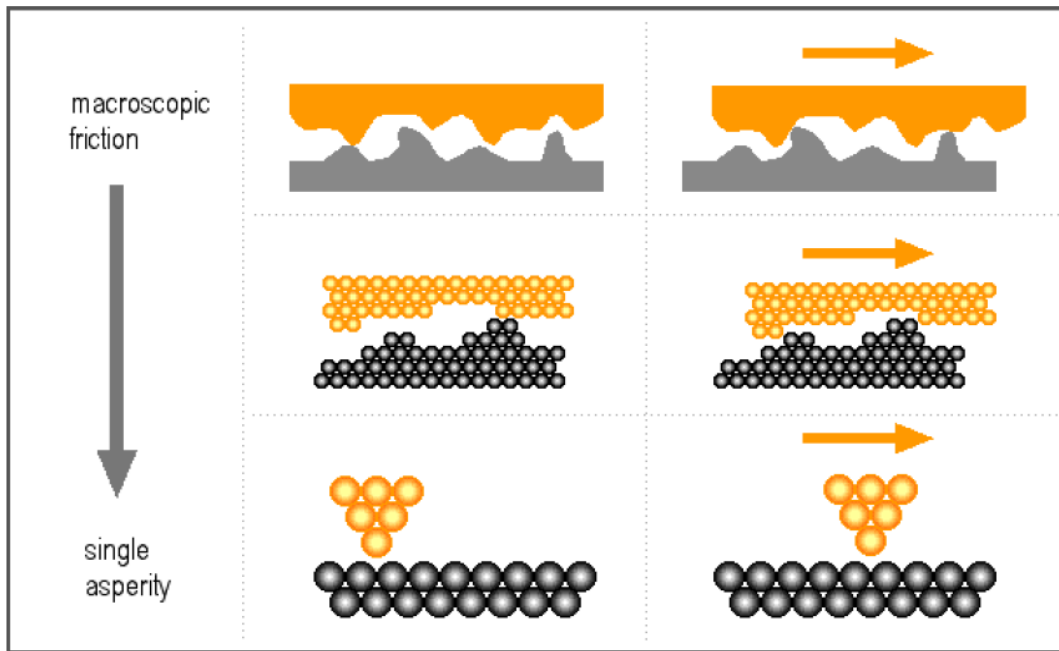


Friction at the nanoscale can be inferred from such measurements



- $(A+B)-(C+D) = \text{normal force (AFM signal)}$
- $(A+C)-(B+D) = \text{lateral force (LFM signal)}$

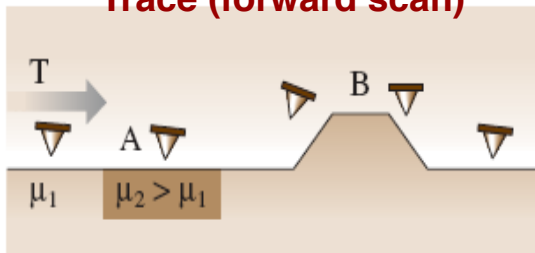
# NANOTRIBOLOGY



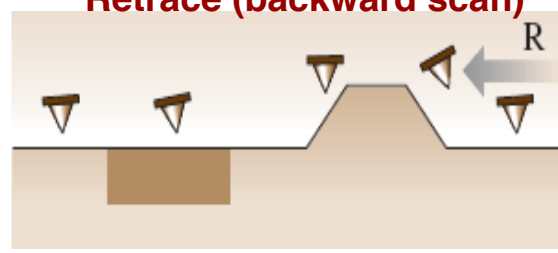
Sliding motion of the AFM tip “**in contact**” with the surface turns out affected by “tribological mechanisms” at the atomic scale:

- **Adhesion;**
- **Ploughing;**
- **Deformation**

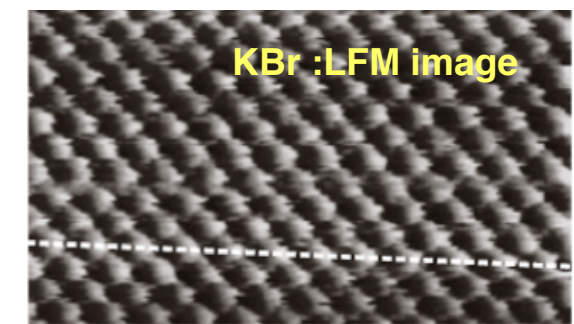
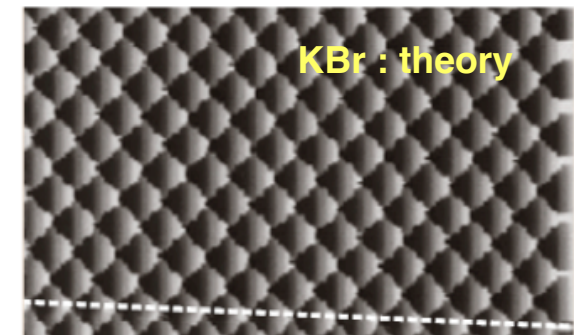
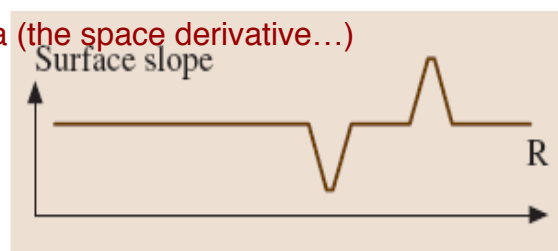
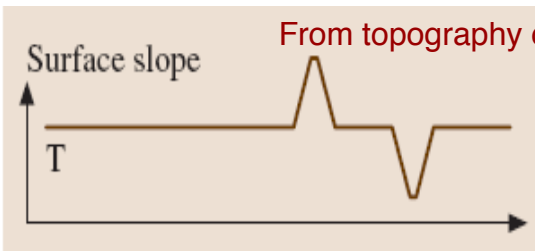
**Trace (forward scan)**



**Retrace (backward scan)**

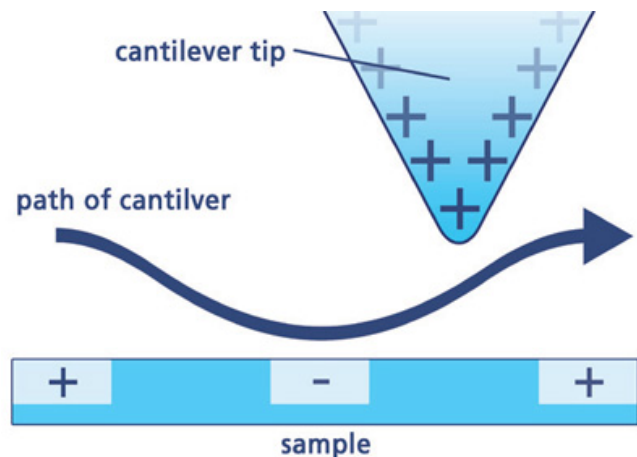


From topography data (the space derivative...)

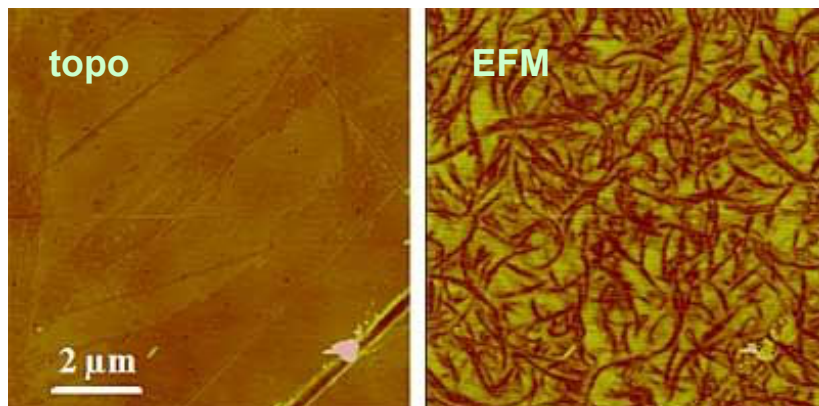
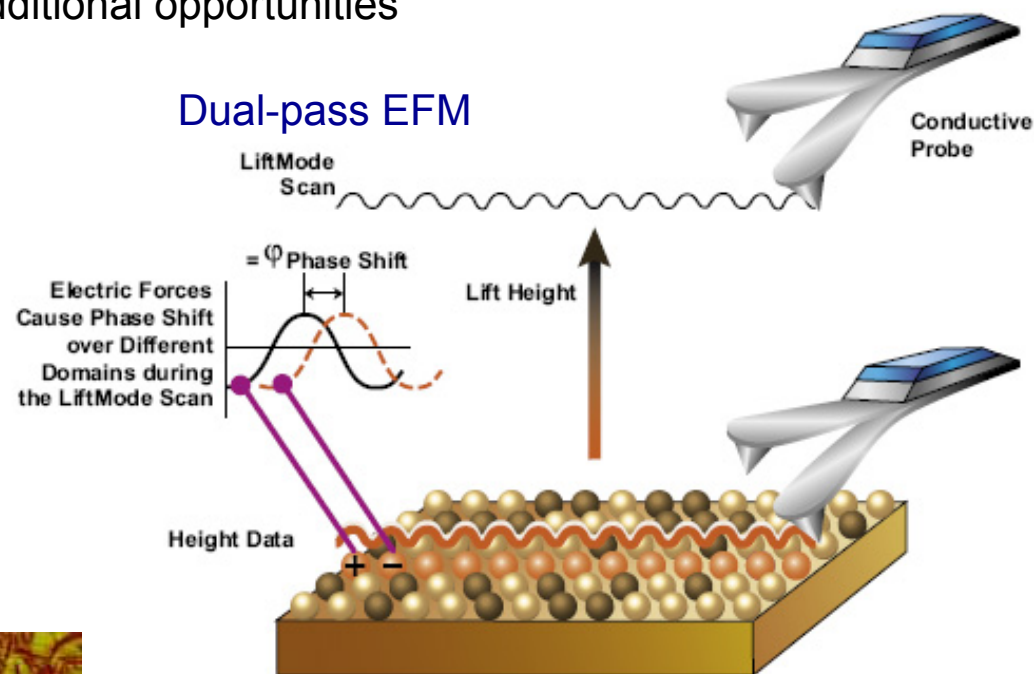


# ELECTROSTATIC FORCE MICROSCOPY (EFM)

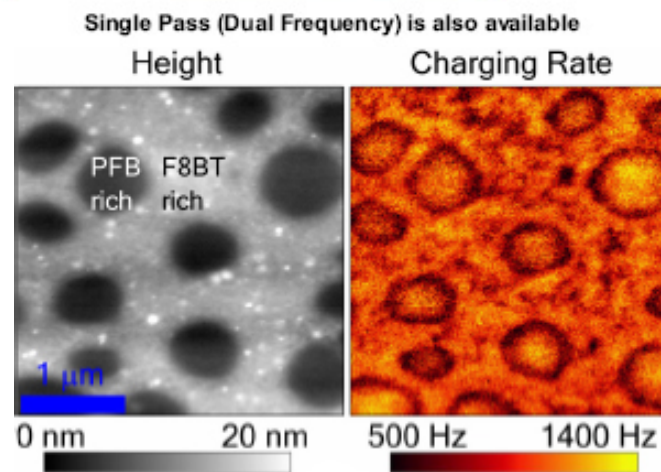
Electrical polarization of the tip opens additional opportunities



## Dual-pass EFM

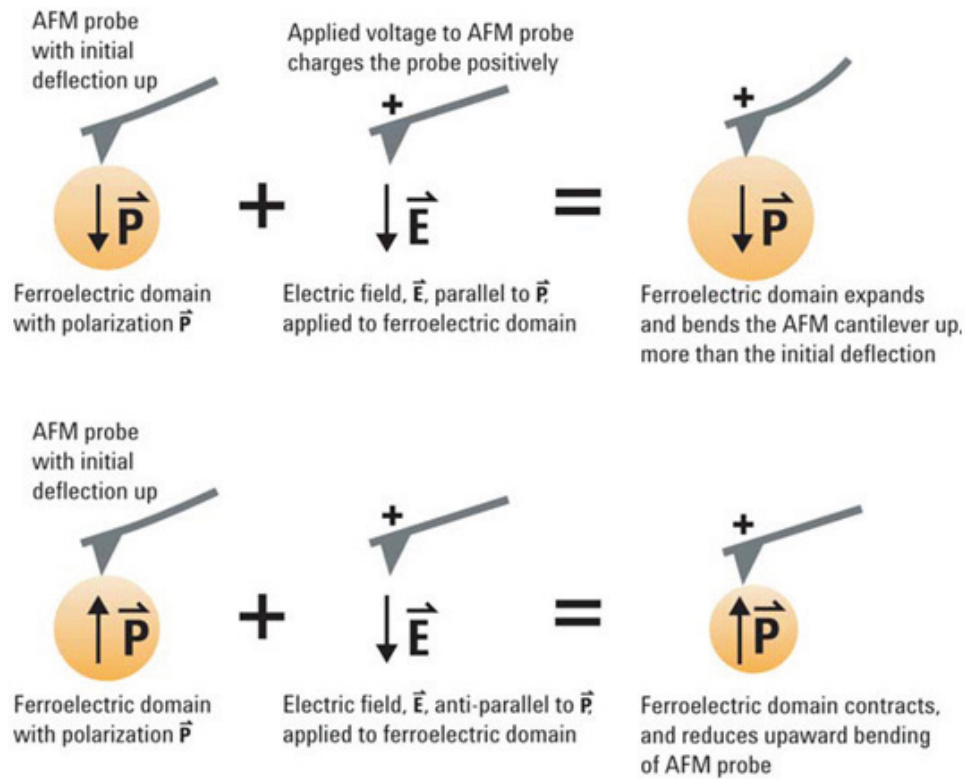


CNT dispersed in polyimide  
(NIST 2010)

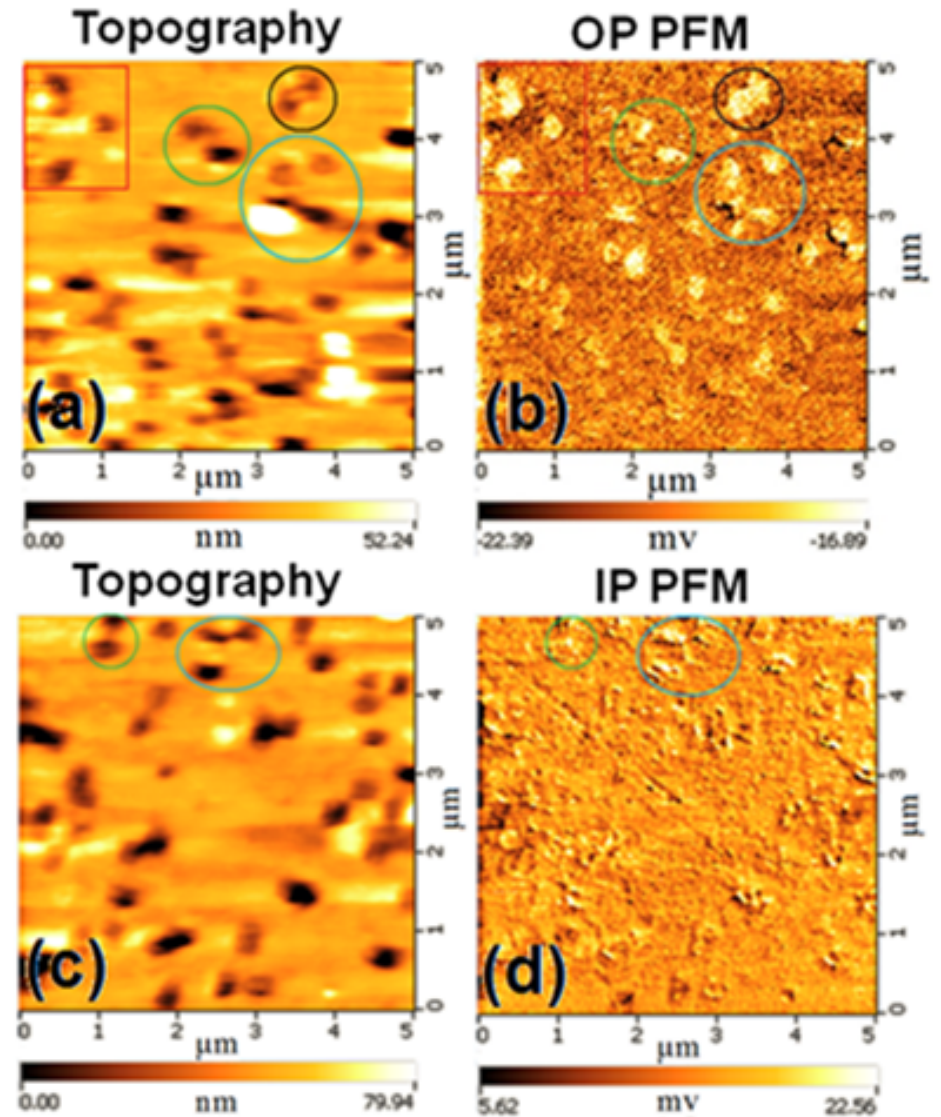


DOI: 10.1117/2.1200702.0636

# PIEZOELECTRIC FORCE MICROSCOPY (PFM)



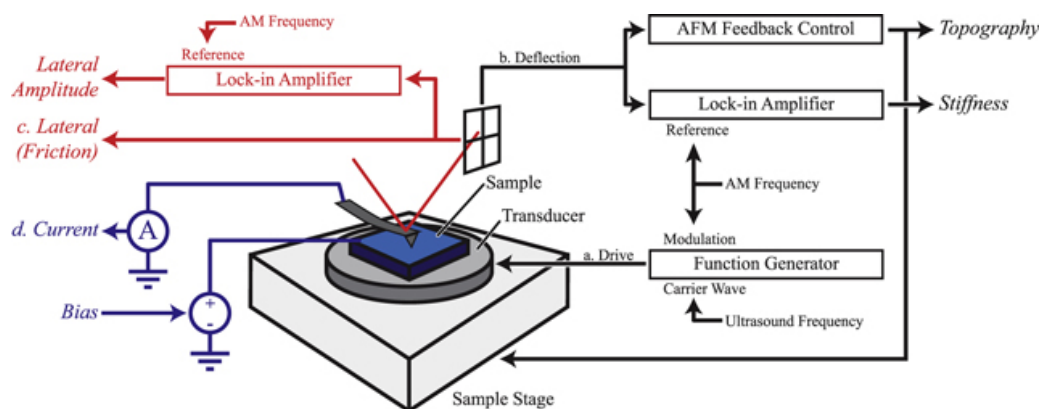
BFM (Bi-containing iron oxide) thin films



DOI: 10.5772/52519

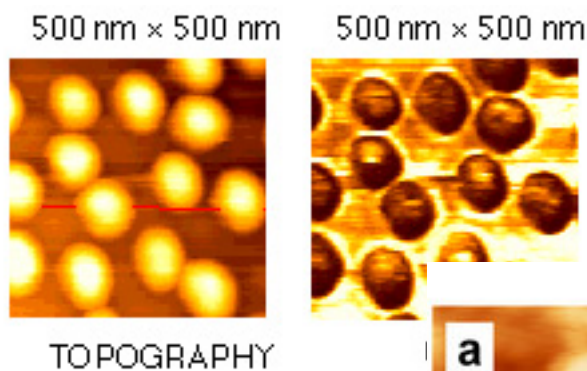


# ULTRASONIC FORCE MICROSCOPY (UFM)



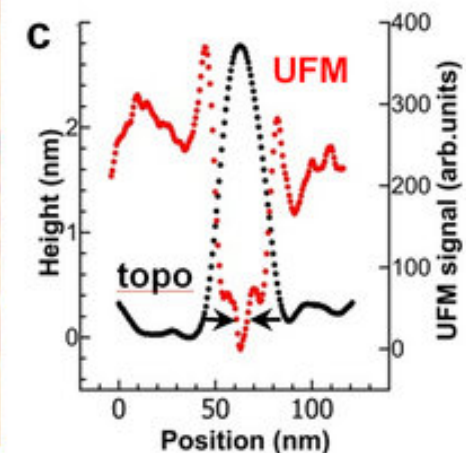
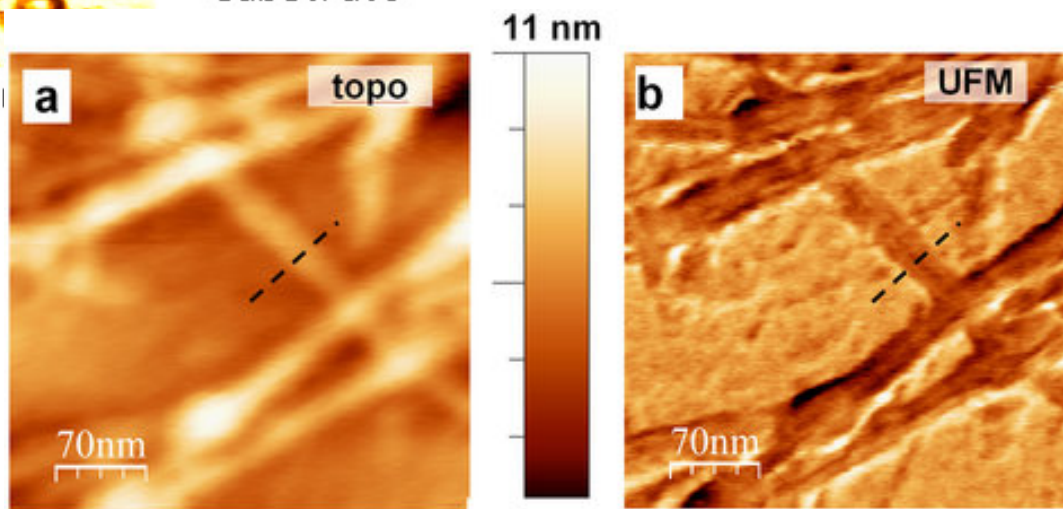
Fast (“ultrasonic”) oscillation of the sample induces a sort of intermittent contact

Since perturbation is applied from the bottom, the material volume and in particular the interfaces are sensed



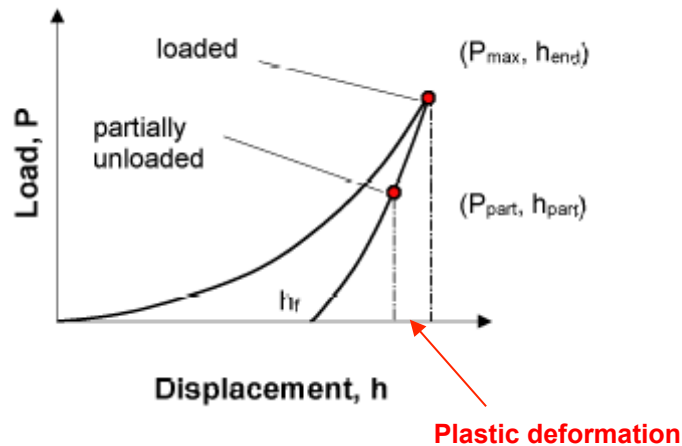
Ge quantum dots on Si (100) substrate

Aggregated peptides



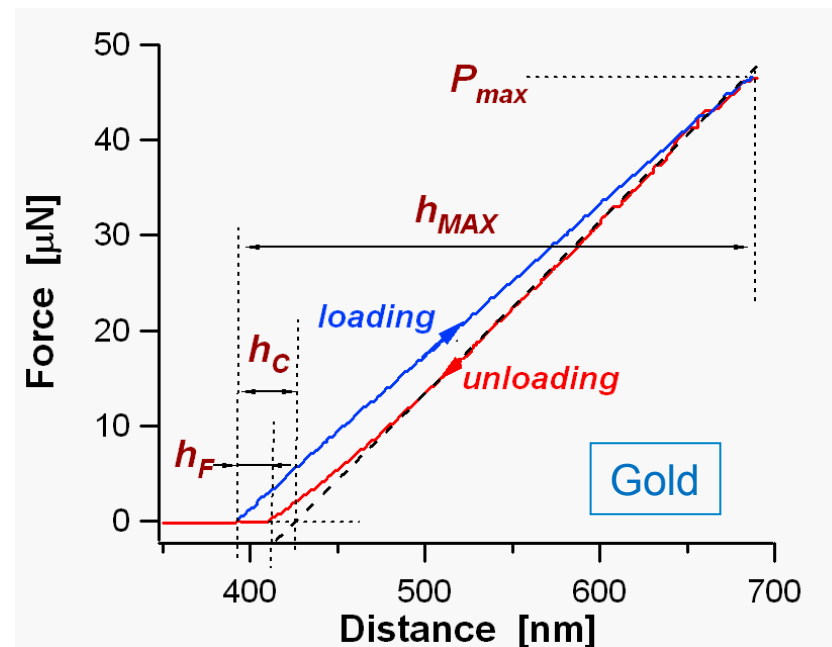
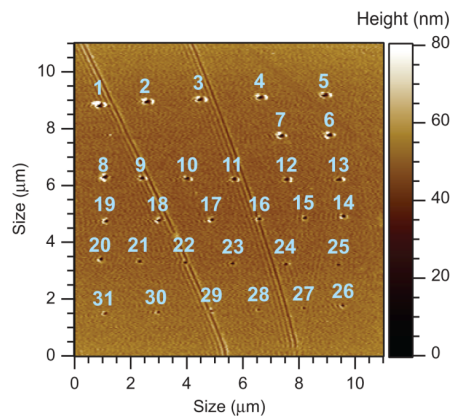
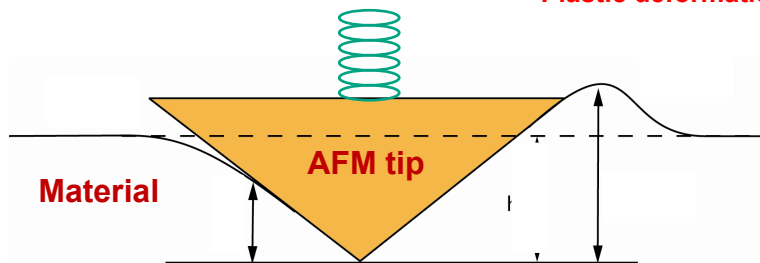
doi:10.1038/srep04004

# NANOINDENTATION I



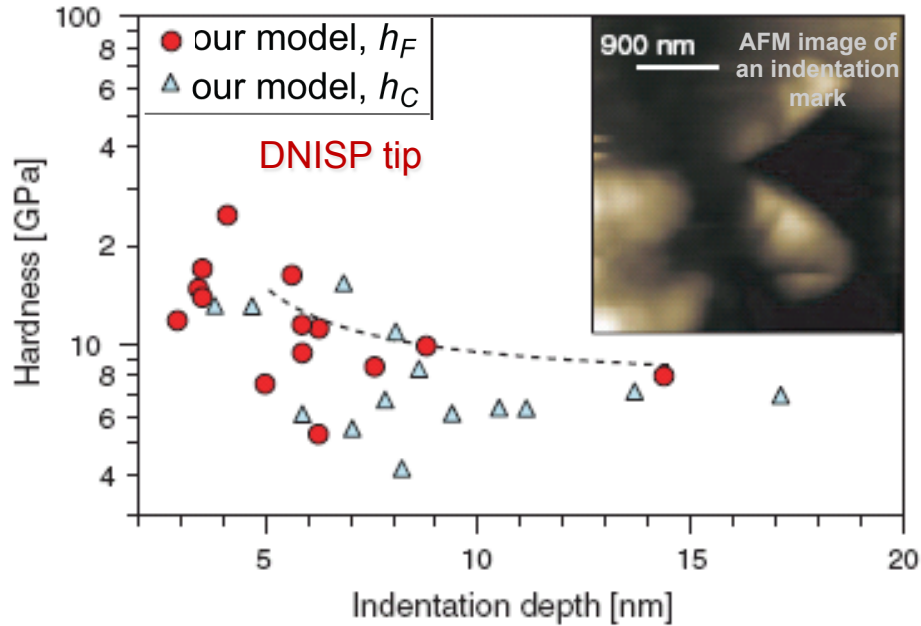
(Nano)indentation is a common technique to ascertain elastic/plastic behavior of the materials (if carried out with a load modulation, also surface viscoelasticity can be analyzed)

Data pertaining to the elastic modulus and to the plastic behavior (e.g., shear modulus) can be attained and comparison with macroscopic results (e.g., Vickers hardness, Rockwell,...) may lead to interesting insights on the microscopic nature of surfaces and nanostructures



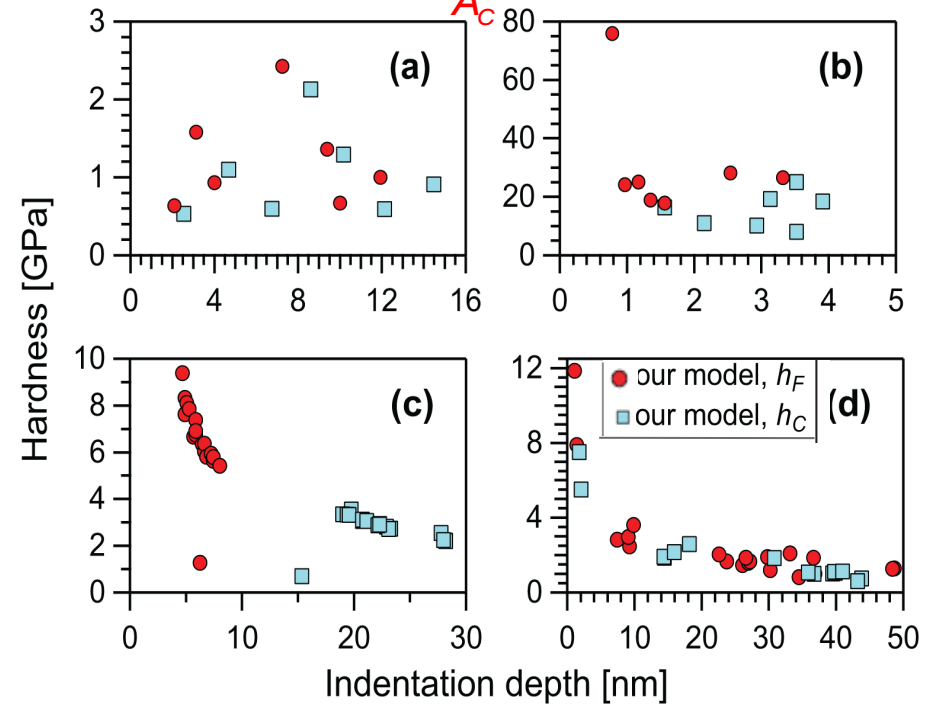
# NANOINDENTATION II

## Nanoindentation of a hard coating (BALINIT C)



Material	Investigated depth range [nm]	$a$	$H_0$ [GPa]	Literature data [GPa]
Silicon	0.5-4.0	-1.9	13±2.4	13
Gold	5-28	-1.3	1.3±0.2	1.1-1.4
Balinit C	2-15	-1.0	5.5±1.2	5-8 (?)
Polystyrene	3.0-10	-1.2	0.83±0.22	~0.3
PMMA	1.0-30	-0.73	0.58±0.16	~0.4

Material hardness:  $H = \frac{P_{MAX}}{A_C}$



- (a) Aluminium Bulk DNISP
- (b) Silicon Wafer DNISP
- (c) Polystyrene Layer DDESP
- (d) PMMA Layer DDESP

Layers are 100 nm thick spin coated films on glass

Apparently, hardness increases for nanosized indentation

# CONCLUSIONS

- ✓ Technical advancements (tips and piezoscanners) combined with some great ideas (the feedback) enabled the development of “smart” and quite effective scanning probe microscopies
- ✓ In general terms, the goodies of such SPMs are in the extreme spatial resolution joined with the capability to carry out, quite often, quantitative measurement of local physical quantities
- ✓ In that, SPMs represent a breakthrough compared to conventional high resolution microscopy, e.g., SEM/TEM, where, even in the presence of strong contrast mechanism, measurements other than morphology/structure are usually prevented, or made cumbersome
- ✓ STM, the “mother of all SPMs”, provides with an excellent resolution, but in a restricted range of applications
- ✓ AFM is a much more developed and diffused technique, able to operate in a variety of configurations and operating modes in order to access different material properties

*We have not lost our “optical spectroscopy” reference, though:  
we will come back to that in the next lecture,  
where optics and SPM will be combined together*

## FURTHER READING

For a very well done overview of quantum physics phenomena, including tunneling:

R. Eisberg, R. Resnick, Quantum Physics of Atoms, Molecules, ..., Second Edition, Wiley, New York (1985).

For a reference on the Nobel Prize in Physics, 1986:

[https://www.nobelprize.org/nobel\\_prizes/physics/laureates/1986/press.html](https://www.nobelprize.org/nobel_prizes/physics/laureates/1986/press.html)

For a basic information on AFM in nanotechnology:

R. Waser, Ed., Nanoelectronics and information technology, Wiley, New York (2003).

For a review on SPM, with a gallery of images and practical information:

<http://www.ntmdt-si.com/page/resources>